



TAMPERE UNIVERSITY OF TECHNOLOGY

CHENGYAN SUN

HYDROSTATIC-MECHANICAL POWER SPLIT CVT

Master of Science Thesis

Examiners: Professor Kalevi Huhtala  
Msc. Janne Uusi-Heikkilä

Examiner and topic approved at the faculty  
council meeting of Automation, Mechanical  
and Materials engineering on 8th of  
September 2010

## Abstract

TAMPERE UNIVERSITY OF TECHNOLOGY

Master's Degree Program in Machine Automation

CHENGYAN, SUN: Hydrostatic-Mechanical Power Split CVT

Master of Science Thesis, 52 pages, 6 Appendix pages

January 2011

Major: Mechatronics

Examiners: Professor Kalevi Huhtala, Msc. Janne Uusi-Heikkilä

Keywords: hydrostatic, mechanical, power split, CVT, Planetary, steady state characteristics, application, transmission efficiency, work cycle suitability, power range suitability

The customer requirements of low fuel consumption, low emissions, and high performance require new technical solutions allowing for optimization of the entire drive train, CVT technology, continues to emerge as a key technology for improving the fuel efficiency of vehicle with internal combustion engines, because it allows the engine to operate at peak efficiency and reduces the operation difficulty. Hydrostatic-mechanical power split CVT is a special CVT technology, it is suitability for high power density applications. It lies in between the pure hydrostatic and the pure mechanical transmissions.

This thesis involved the study of the hydrostatic-mechanical power split CVT technology. Based on the theoretical model, the steady state characteristics were studied to display the advantage and disadvantage of this transmission, then a market application review was made to show the practical application of this technology, finally suitability study was carried out based on dynamic model, to find out the working cycle suitability and power range suitability of this transmission technology.

## Preface

I would like to thank Professor Kalevi Huhtala for the interesting topic he provided, and his useful suggestions. I would like to extend my gratitude to Msc. Janne Uusi-Heikkilä for his wise counsel and constructive comments. A special thanks to Dr. Mikko Erkkilä for providing me useful materials and warm help.

In addition, I would like to thank my parents, for their love, effort and guidance to make me a thoughtful man. Finally, I would like to thank my love Qiu Dan, for her love, which makes my life wonderful and promising.

Chengyan Sun

Tampere, 2011

## Table of Contents

Nomenclature.....	i
1 Introduction.....	1
1.1 Background .....	1
1.2 Object .....	2
1.3 Structure of the thesis.....	2
2 Fundamental theory .....	3
2.1 The principle of hydrostatic-mechanical power split CVT .....	3
2.2 Classification of the hydrostatic mechanical power split CVT .....	4
2.3 The components of the hydrostatic mechanical power split CVT .....	5
3 Steady state modeling of basic power split circuit.....	6
3.1 Input coupled circuit .....	6
3.1.1 Power flow .....	6
3.1.2 Power distribution diagram .....	7
3.1.3 Input coupled model.....	8
3.2 Output coupled .....	11
3.2.1 Power flow .....	11
3.2.2 Power distribution diagram .....	13
3.2.3 Output coupled model.....	14
3.3 The variable bridge transmission .....	16
3.4 Steady state hydrostatic transmission models .....	16
3.4.1 Pump model .....	16
3.4.2 Motor model .....	17
3.5 Summary .....	18
4 Steady State Characteristics .....	19
4.1 Input coupled speed summation .....	19
4.2 Output coupled simulation .....	22
4.3 Summary .....	25
5 HMPS-CVT Application .....	26
5.1 The Claas-Jarchow HM-8 and HM-II.....	26
5.2 The Fendt Vario .....	27
5.3 The Steyr S-Matic for Steyr, Case, New Holland .....	29
5.4 The ZF Eccom for Deutz-Fahr, John Deere, Claas .....	30
5.5 Yanmar CVT .....	32

5.6	Summary .....	34
6	Suitability study.....	35
6.1	Diesel engine .....	35
6.2	Model of hydrostatic transmission .....	36
6.3	Tire road connection .....	38
6.4	Drive wheel model.....	38
6.5	Vehicle dynamics .....	39
6.6	Powertrain model .....	40
6.7	The powertrain simulation examples.....	41
6.8	The working cycle suitability .....	43
6.9	The power range suitability study .....	46
6.10	Conclusion.....	48
7	Summary .....	49
	References .....	50
	Appendix: Simulink models.....	53

Figure 2.1 Power split CVT .....	3
Figure 2.2 Input coupled circuit .....	4
Figure 2.3 Output coupled circuit .....	4
Figure 2.4 Variable bridge .....	5
Figure 2.5 Planetary gear (Yuliang Leon Zhou 2005) .....	5
Figure 3.1 Non-regenerative of input coupled circuit.....	6
Figure 3.2 Regenerative of input coupled circuit.....	7
Figure 3.3 Possible power flow of input coupled circuit .....	7
Figure 3.4 Power flow diagram of input coupled .....	8
Figure 3.5 Input coupled model .....	9
Figure 3.6 Input coupled block diagram .....	10
Figure 3.7 Non-regenerative of output coupled .....	11
Figure 3.8 Regenerative of output coupled circuit.....	12
Figure 3.9 Possible power flow of output coupled .....	12
Figure 3.10 Power distribution diagram of output coupled .....	13
Figure 3.11 Input coupled model .....	14
Figure 3.12 Input coupled block diagram .....	15
Figure 3.13 Variable bridge transmission .....	16
Figure 4.1 Input coupled driveline schematic (Ivantysynova Monika 2010) .....	19
Figure 4.2 Pump and motor displacement setting.....	20
Figure 4.3 Input coupled drive diagram.....	21
Figure 4.4 Input coupled power transmission diagram.....	21
Figure 4.5 Output coupled driveline (Ivantysynova Monika 2010).....	22
Figure 4.6 Pump and motor displacement settings .....	23
Figure 4.7 Drive diagram of output coupled driveline.....	23
Figure 4.8 Power transmission diagram of output driveline .....	24
Figure 5.1 Efficiency target for CVT of larger tractors above 100kW (Renius 1999) ...	27
Figure 5.2 Fent Vario for the tractor Favorit (1996).....	27
Figure 5.3 Transmission characteristics of input coupled (Renius, K. Th. and Resch, R. 2005) .....	28
Figure 5.4 Transmission characteristics (Renius, K. Th. and Resch, R. 2005).....	28
Figure 5.5 The S-Matic hydrostatic power split CVT (Zbigniew Żebrowski 2007) .....	29
Figure 5.6 Tractor drive diagram (Zbigniew Żebrowski 2007) .....	30
Figure 5.7 Efficiency diagram (Aitzetmüller Heinz 2000) .....	30
Figure 5.8 ZF - Eccom hydrostatic-mechanical power split CVT (Zbigniew Żebrowski 2007 ) .....	31
Figure 5.9 Hydrostatic power portions and speed of first left sun gear within the 4 ranges (Pohlenz and Gruhle 2002) .....	32
Figure 5.10 Yanmar CVT (Renius, K. Th., Resch, R 2005).....	33
Figure 6.1 Engine power curve (Daiheng Ni 2008).....	36
Figure 6.2 Engine power curve (Daiheng Ni 2008).....	36
Figure 6.3 Dynamic model of the hydrostatic transmission .....	38
Figure 6.4 Drive wheel illustration .....	39
Figure 6.5 vehicle dynamics .....	40

Figure 6.6 Powertrain model.....	41
Figure 6.7 Pump displacement setting .....	42
Figure 6.8 Vehicle velocity response .....	42
Figure 6.9 Engine speed control signal .....	43
Figure 6.10 Vehicle velocity response .....	43
Figure 6.11 Typical hybrid vehicle working cycle .....	44
Figure 6.12 Powertrain simulation working cycle .....	44
Figure 6.13 Powertrain efficiency curve .....	45
Figure 6.14 Powertrain velocity response .....	45
Figure 6.15 Power range suitability curve .....	47
Table 3.1 Transmission ratio and transmission type of Input coupled circuit .....	8
Table 3.2 Transmission ratio and transmission type of Output coupled circuit .....	13
Table 4.1 Input coupled driveline simulation parameters .....	19
Table 4.2 Output coupled simulation parameters .....	22
Table 6.1 Powertrain simulation parameters.....	41
Table 6.2 Powertrain control parameters .....	42
Table 6.3 Working cycle simulation parameters.....	44
Table 6.4 Eaton vehicle performance.....	46
Table 6.5 Transmission suitability study result.....	46

## Nomenclature

$B$	Oil bulk modulus
$C_1, C_2, C_3$	Constant
$CVT$	Continuously variable transmission
$e$	Constant
$F_a$	Acceleration force
$F_f$	Friction force
$F_l$	External load force
$F_t$	Traction force
$HMPSCVT$	Hydrostatic-mechanical power split CVT
$IC$	Internal combustion
$ICE$	Internal combustion engine
$i_{FR}$	Speed ratio between output shaft and drive wheel
$k_1, k_2, k_3, k_4$	Coefficient
$k_{hm}$	Speed ratio between output shaft and hydraulic motor
$k_m$	Speed ratio between output shaft and engine
$k_{mp}$	Speed ratio between pump and output shaft
$k_p$	Speed ratio between pump and engine
$M_e$	Engine torque
$M_{fr}$	Drive torque
$M_{fw}$	Friction torque
$M_{fw0}$	Coulomb friction torque
$M_{hm}$	Hydraulic motor torque
$M_{lm}$	Hydro-mechanical torque loss
$M_{lp}$	Pump torque loss
$M_m$	Mechanically transmitted torque
$M_p$	Pump torque
$M_{pa}$	Available pump torque
$MR$	Mechanical power regenerative
$N$	Normal force
$NR$	Non-regenerative
$n_c$	Rotational speed of the carrier of the planetary gear
$n_r$	Rotational speed of the ring gear of the planetary gear
$n_s$	Rotational speed of the sun gear of the planetary gear
$P_h$	Power portion of the hydrostatic path
$P_i$	Input power
$P_m$	Power portion of the mechanical path
$P_{max}$	Maximum engine power
$P_o$	Output power
$Q_{lm}$	Leakage flow of motor
$Q_{lp}$	Leakage flow of pump
$Q_m$	Motor flow
$Q_p$	Pump flow
$r$	Drive wheel radius
$R$	Ring gear teeth number
$R_t$	Transmission ratio in the mechanical path of the planetary gear
$R_{tl}$	Transmission ratio at the lockup point



$S$	Sun gear teeth number
$S_l$	Slip between tire and road
$T$	Engine torque
$T_{max}$	Maximum engine torque
$V$	Absolute velocity of the vehicle
$V_r$	Circumferential velocity of the tire
$\Delta P$	Pressure difference
$\varepsilon_p$	Pump displacement setting
$\varepsilon_m$	Motor displacement setting
$\omega_c$	Planetary carrier angular velocity
$\omega_e$	Engine angular velocity
$\omega_{es}$	Set engine angular velocity
$\omega_{hm}$	Motor angular velocity
$\omega_{in}$	Input angular velocity
$\omega_m$	Angular velocity of mechanical path
$\omega_{out}$	Output angular velocity
$\omega_p$	Pump angular velocity
$\omega_{pp}$	Engine speed at the maximum power
$\omega_{pt}$	Engine speed at the maximum torque
$\omega_w$	Wheel angular velocity
$\eta$	Overall efficiency

# 1 Introduction

Nowadays development trends in car industry and mobile machines are driven by global concerns on energy limitation and greenhouse gases reduction, more energy efficient and environmentally friendly vehicles will be needed. It was reported that the 50% improvement of fuel efficiency contributes to 33% reduction of CO<sub>2</sub> gas. (Heera Lee 2003). Therefore, improvement of the fuel efficiency can be considered to be of vital importance to meet the requirement for the emission reduction as well as the fuel economy.

## 1.1 Background

After more than a century of research and development, the internal combustion engine (ICE) is nearing perfection, though engineers continue to explore the outer limits of internal combustion (IC) efficiency and performance, advancements in fuel economy and emissions have effectively stalled (Kevin R. Lang 2000). With limited room for improvement, vehicle manufacturers have begun full scale development of alternative power vehicles. A feasible solution to improve fuel efficiency is to further optimize the overall efficiency of internal combustion vehicles. One of the possible approaches is to adopt continuously variable transmission (CVT), because a CVT continuously changes its gear ratio to optimize engine efficiency, so that allows the engine to operate at peak efficiency with a perfectly smooth torque-speed curve. Though CVTs are not new technology, limited torque capabilities, poor reliability and the poor control schemes have inhibited their growth.

In order to improve the CVT's capacity, efficiency, and durability, many different types of CVT have been developed in the past decades. Hydrostatic-Mechanical Power Split CVT is a very special type of CVT, which was being developed as a prime propulsion technology in very high power density applications. It lies in between the pure hydrostatic and the pure mechanical transmissions, and the proper coupling of these two kinds of transmission technology will result in outstanding performance that retains most of the advantages of both mechanical and hydrostatic transmissions. This thesis is to investigate hydrostatic-Mechanical Power Split CVT circuits' models and analysis their suitability.

## 1.2 Object

This thesis aims to investigate Hydrostatic-Mechanical Power Split CVT (HMPSCVT) circuits' models and analysis the suitability of this technology. The objectives are summarized as:

- Study the characteristics of the hydrostatic-mechanical power split CVT
- Study the behaviors of basic circuits
- Study the power flow of hydrostatic-mechanical power split CVT
- Study dynamic behavior of the hydrostatic-mechanical power split CVT
- Study the suitability of the hydrostatic-mechanical power split CVT

## 1.3 Structure of the thesis

The thesis is divided into 7 chapters as:

- 1) Chapter 1 gives an introduction on the technology, introduce the background, object and structure of the thesis.
- 2) Chapter 2 reviews the current research about the technology.
- 3) Chapter 3 presents the steady state characteristics of the circuits.
- 4) Chapter 4 studies the behavior of the circuits.
- 5) Chapter 5 reviews the current industry applications of this kind of technology.
- 6) Chapter 6 studies the suitability of this technology.
- 7) Chapter 7 gives the final summary of the thesis.

## 2 Fundamental theory

This chapter reviews the principle of the hydrostatic-mechanical power split CVT, demonstrates its advantages, then lists its classification and the basic configurations of each type, at the end of this chapter is the components used in the hydrostatic-mechanical power split CVT transmission.

### 2.1 The principle of hydrostatic-mechanical power split CVT

According the James H. Kress (Kress James H. 1968) the definition of Hydrostatic-Mechanical Power Splitting transmission is: An energy translation device in which mechanical energy at the input is converted into mechanical and hydrostatic energy and then is reconverted into mechanical energy before leaving at the output. Figure 1 demonstrates the basic principle structure of a hydrostatic mechanical power split drive.

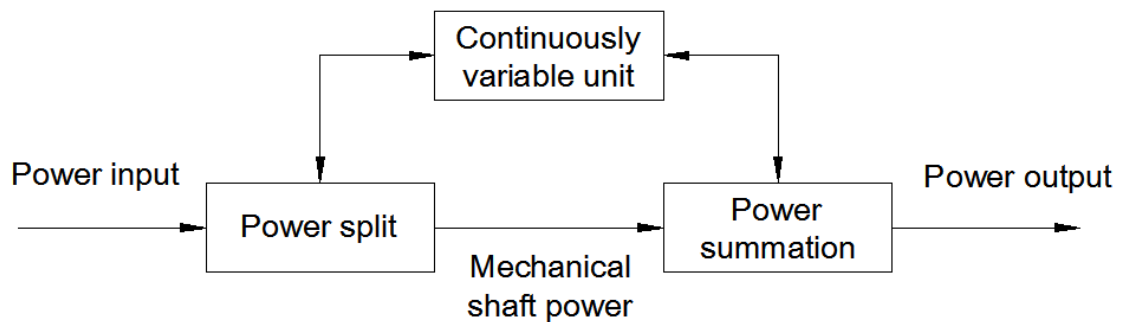


**Figure 2.1** Power split CVT

The basic idea is to split the input power into two parts, with one part of the power send through a variable ratio hydrostatic path, with the remainder part of the power into a constant ratio mechanical path with higher efficiency. The two part of power are then summed up in a mechanical differential gear or planetary gear.

For a given input speed  $\omega_{in}$ , two velocities are added at the planetary gear, with one fixed and the other variable, thus the output speed  $\omega_{out}$  is variable. In accordance with the chosen system design only a part of the transmitted power is transferred via the hydrostatic path (Ivantysynova Monika 2000), and total efficiency is above that of a CVT direct due to the high efficiency by a typical example with realistic values for full power (Renius, K. Th. and Resch, R. 2005).

Assume that a split ratio of 70% with mechanical transmission and 30% with hydrostatic transmission, with a mechanical transmission efficiency of 95%, and a hydrostatic transmission efficiency of 80%. The resulting overall efficiency can be calculated as:

$$0.7 \times 0.95 + 0.3 \times 0.8 = 0.905 = 90.5\%$$

Therefore the overall efficiency benefit increases with decreasing CVT power portion. However in gaining higher efficiency, a reduction in transmission ratio range will be suffered (Norman H. Beachley and Andrew A. Frank 1979).

## 2.2 Classification of the hydrostatic mechanical power split CVT

Hydrostatic-Mechanical Power Split CVT can be divided into three types (Figure 2):

- Input coupled
- Output coupled
- Bridge type

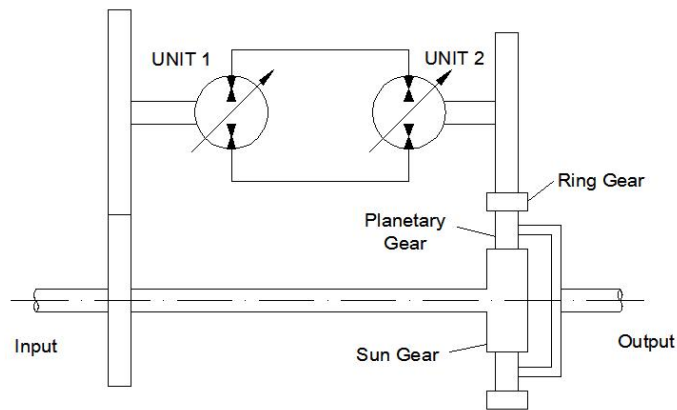


**Figure 2.2** *Input coupled circuit*

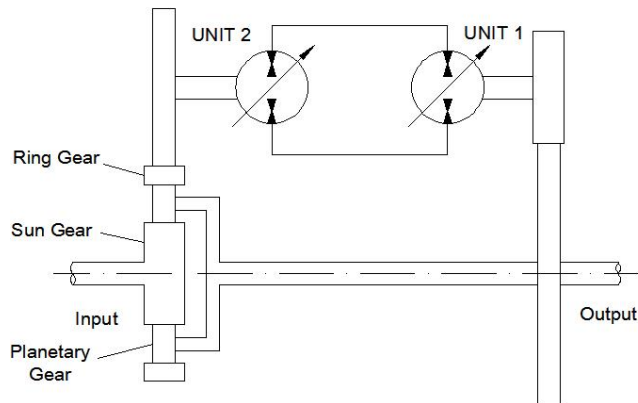


**Figure 2.3** *Output coupled circuit*

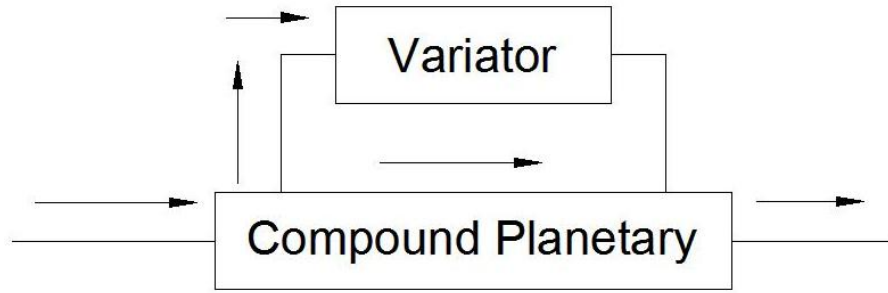


**Figure 2.4** Variable bridge

### 2.3 The components of the hydrostatic mechanical power split CVT

Generally, a power split system consists of three elements: (1) a planetary gear train, (2) a continuous variable unit, (3) a fixed ratio mechanism (FR). The basic elements of a hydrostatic-mechanical power split CVT are:

- Input shaft
- Output shaft
- Planetary Gear Train (PGT)
- CVU
- Internal mechanical transmission

Planetary gears are widely used in many power-split transmissions. Figure 2.5 shows the structure of the planetary gear. It includes a sun gear, a ring gear, and a carrier.

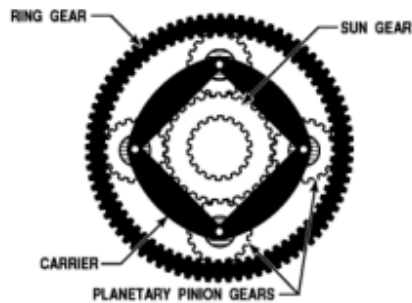


**Figure 2.5** Planetary gear (Yuliang Leon Zhou 2005)

The planetary speed consists three parts, the sun gear speed, the ring gear speed and the carrier speed.

$$n_s S + n_r R = n_c (S + R) \quad (1)$$

Here:

- $n_s, n_r, n_c$  represent rotational speeds of sun gear, ring gear, carrier respectively,
- $S$  and  $R$  are the number of teeth in the sun and ring gear respectively.

### 3 Steady state modeling of basic power split circuit

This chapter aimed to study the theoretical steady state models of the basic HMPS CVT. The models were based on the gear ratios of different parts, the transmission ratio of the hydrostatic path control the power distribution of the whole transmission.

#### 3.1 Input coupled circuit

Input coupled is also synonymous for split torque. The layout of input coupled circuit implies that one of the hydraulic units is attached to input shaft. Split torque refers to that the input torque is split into two parts, and transmitted by hydrostatic and mechanical path. The rotational speeds of the CVU and the mechanical drive are summed up at the planetary and finally transmitted to the drive shaft.

##### 3.1.1 Power flow

The famous paper of Kress (Kress James H. 1968) contains the complete models input and output coupled systems. The transmission lockup point is a point at which a power-split CVT transmission becomes purely mechanical (P. Linares 2010). At the lockup point the floating shaft of the planetary gear train is being stationary, the mechanical path transmission in this point is known as lockup ratio. Up to the lockup ratio a condition occurs in which the ring gear of the planetary gear train is driven by hydraulic unit 2, which acts as a motor. In this region, power circulation is said to be non-regenerative in which no power feedback occurs through the system as shown in Figure 3.1 Thus, this can be a favorable operating zone.

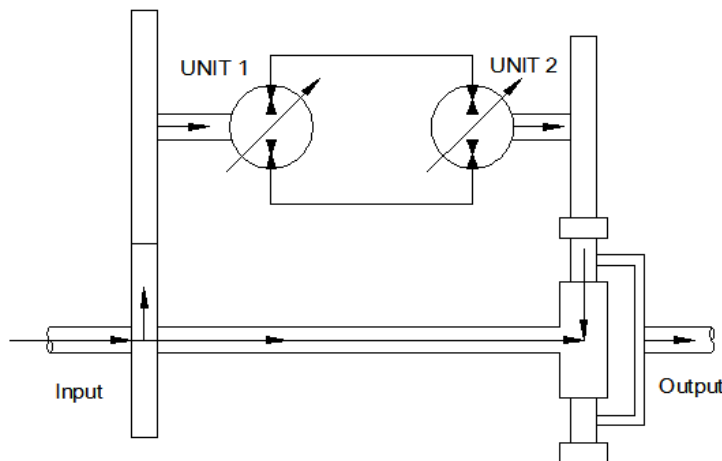


**Figure 3.1** Non-regenerative of input coupled circuit

From the lockup ratio on a condition occurs in which the floating shaft of the planetary train drives the hydraulic unit 2, which acts as a pump. Power is feed back to

hydraulic unit 1 which under this condition acts as a motor, and power is added to the input power as shown in Figure 3.2. Power circulation is regenerative in this region.

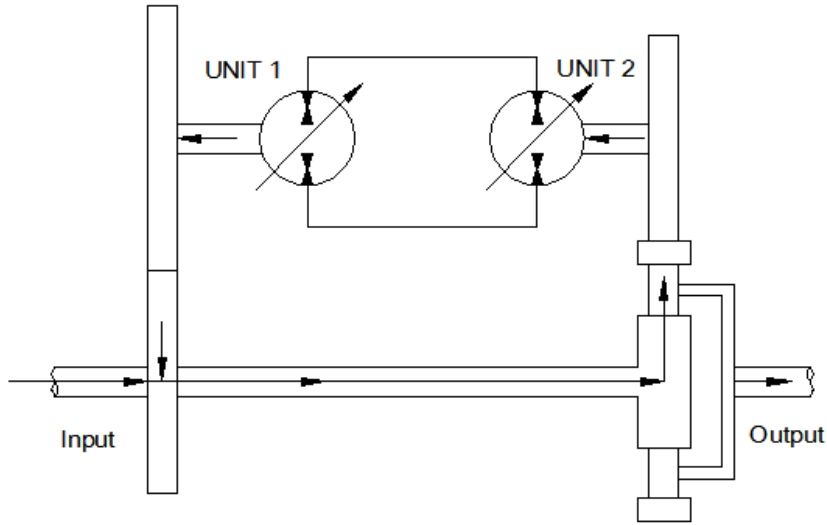


**Figure 3.2** Regenerative of input coupled circuit

The following diagram shows the possible patterns of power flows of input coupled circuit:

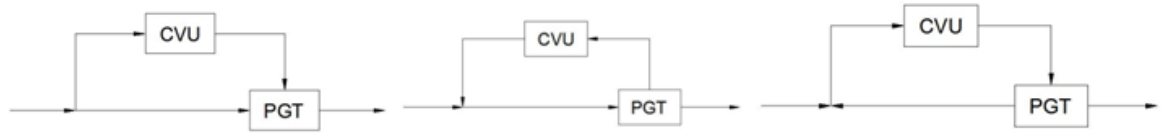


**Figure 3.3** Possible power flow of input coupled circuit

Once the lockup point transmission ratio is known, the distribution of power and its status can be determined:

- Transmission ratio in the mechanical path of the planetary gear train  $R_t$
- Transmission ratio at the lockup point  $R_{tl}$
- The power portion in the hydrostatic path  $P_h$
- The power portion in the mechanical path  $P_m$

$$P_h = 1 - \frac{R_{tl}}{R_t} \quad (2)$$

$$P_m = \frac{R_{tl}}{R_t} \quad (3)$$

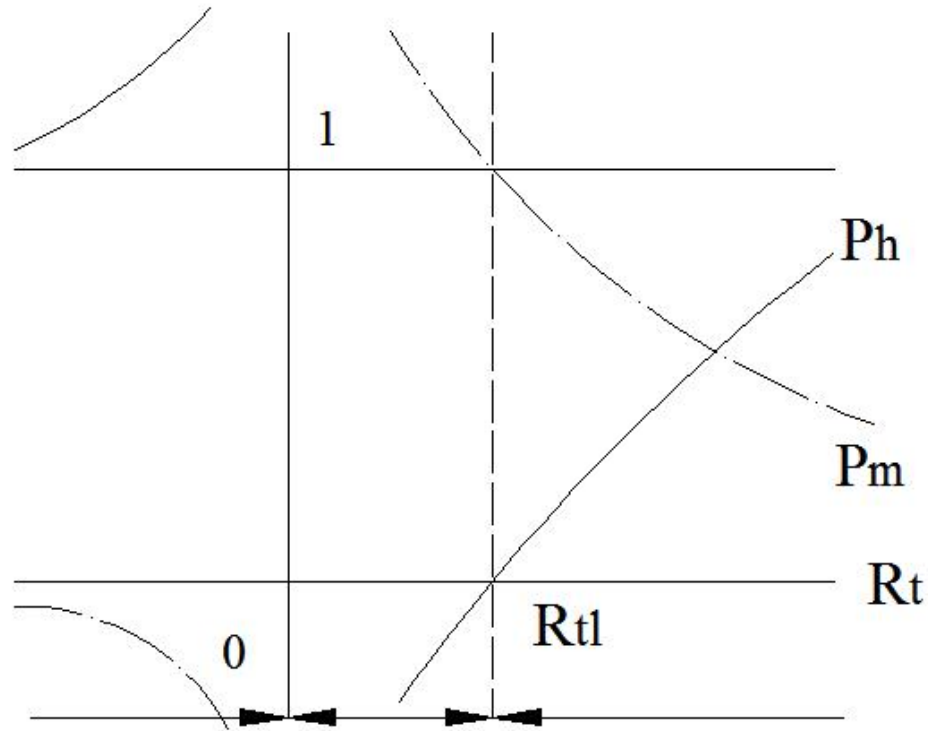
### 3.1.2 Power distribution diagram

It is possible to determine the type of the transmission: Non-regenerative (NR), Mechanical regenerative (MR), and Variable unit regenerative (VR) according to the transmission ratio  $R_t$ .



**Table 3.1** Transmission ratio and transmission type of Input coupled circuit

Transmission ratio $R_t$	Transmission type	Hydraulic power portion $P_h$
$R_t < 0$	VR	$P_h > 1$
$0 < R_t < R_{tl}$	MR	$P_h < 0$
$R_t > R_{tl}$	NR	$0 < P_h < 1$

**Figure 3.4** Power flow diagram of input coupled

### 3.1.3 Input coupled model

In input coupled circuit as shown in Figure 3.5, the prime mover or the engine drives the sun gear of the planetary and the hydraulic pump. The hydraulic motor drives the ring gear of the planetary gear. The torque of the engine is divided into two parts, and transmitted via hydrostatic path and mechanical path. The speed of the output shaft is the speed summation of the two paths.

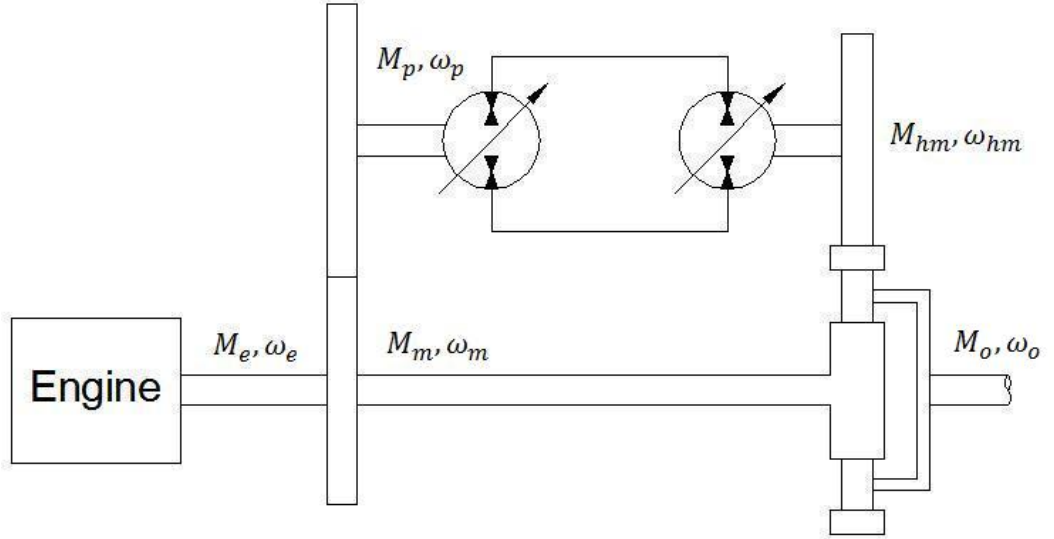


**Figure 3.5** Input coupled model

In the beginning of the operation, the pump is at zero displacement, while the motor is at the maximum displacement, the power at this point is transmitted totally by mechanical path. Then the pump displacement increases in the positive direction, as a result the ratio of the hydrostatic transmission is increased, the output speed is increased as well, the hydraulically transmitted power is added to the mechanically transmitted power.

When the pump displacement is decreased in the negative direction, the hydrostatic path circuits a part of power back to the pump. At the zero output speed operating point, the mechanically transmitted power is totally circuited. This is an unfavorable situation, the design of the transmission should avoid this situation.

According to Mikko Erkkilä (Mikko Erkkilä 2009) the parameters of the input coupled circuit are defined as:

- $\omega_e$  and  $M_e$  are the angular velocity and torque of the engine,
- $\omega_p$  and  $M_p$  are the angular velocity and torque of the pump,
- $\omega_{hm}$  and  $M_{hm}$  are the angular velocity and torque of the hydraulic motor,
- $\omega_m$  and  $M_m$  are the angular velocity and torque of the mechanical path,
- $\omega_o$  and  $M_o$  are the angular velocity and torque of the output shaft,
- $\omega_c$  is the angular velocity of the planetary carrier.

The coefficients are determined as follows:

$$k_1 = \omega_p / \omega_e \quad (4)$$

$$k_2 = \omega_e / \omega_{hm} \quad (5)$$

$$k_3 = \omega_c / \omega_{hm} \quad (6)$$

$$k_4 = \omega_o / \omega_c \quad (7)$$

By combining the equations above, the diagram for the input coupled circuit is derived as

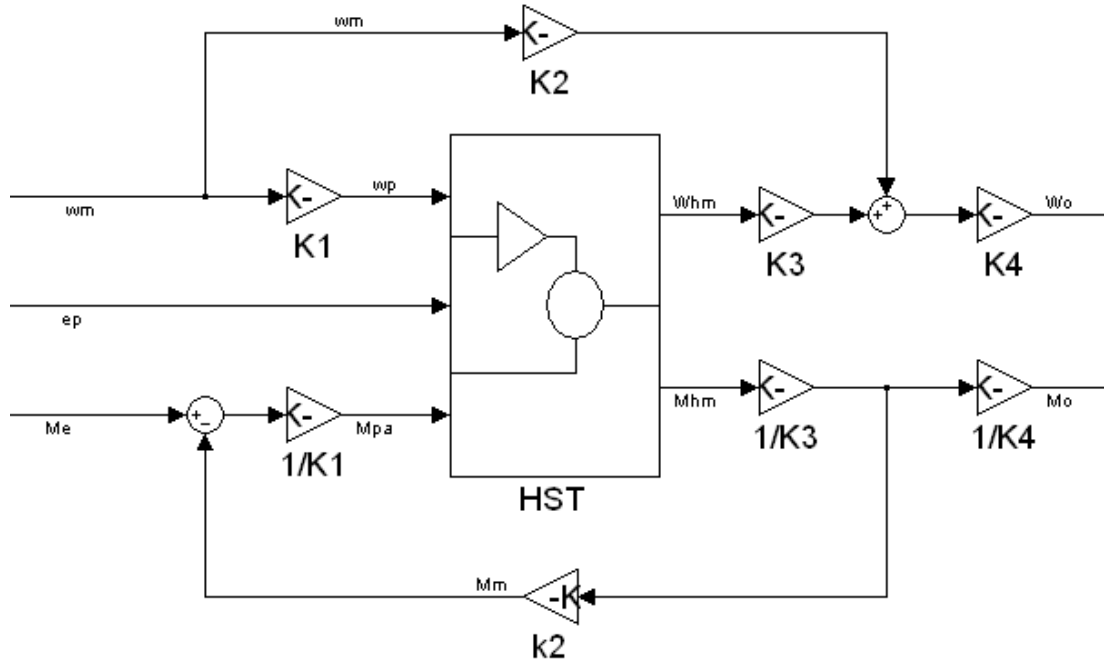


**Figure 3.6** Input coupled block diagram

The pump speed and the available torque:

$$\omega_p = k_1 \omega_e \quad (8)$$

$$M_{pa} = \frac{1}{k_1} \left( M_e - \frac{k_2}{k_3} M_{hm} \right) \quad (9)$$

The output speed and torque:

$$\omega_o = k_4 (k_2 \omega_e + k_3 \omega_{hm}) \quad (10)$$

$$M_o = \frac{M_{hm}}{k_3 k_4} \quad (11)$$

The variable  $M_{pa}$  denotes the available pump torque, and  $M_p$  is the actual pump consumed torque. By determining the speed gear ratios as follows:

$$k_p = \omega_p / \omega_e \quad (12)$$

$$k_m = \omega_o / \omega_e \quad (13)$$

$$k_{hm} = \omega_o / \omega_{hm} \quad (14)$$

The equations of the input coupled circuit are finalized as followings:

$$\omega_p = k_p \omega_e \quad (15)$$

$$M_{pa} = \frac{1}{k_p} \left( M_e - \frac{M_o}{k_m} \right) \quad (16)$$

$$\omega_o = k_{hm} \omega_{hm} + k_m \omega_e \quad (17)$$

$$M_o = \frac{M_{hm}}{k_{hm}} \quad (18)$$

## 3.2 Output coupled

Output coupled is also synonymous for split speed and torque summation. The layout of output coupled circuit implies that one of the hydraulic units is attached to output shaft. Split speed refers to the fact that the input speed is split into two parts, and transmitted by hydrostatic and mechanical path. The torques of the CVU and the mechanical drive summed up at the planetary and finally transmitted to the drive shaft.

### 3.2.1 Power flow

Similarly as the input coupled system, either hydraulic unit can act as a pump or a motor, subtracting power and torque if it acts as a pump, and adding power and torque if it acts as a motor (Kress James H. 1968).

While the mechanical path transmission ratio is smaller than the lockup ratio, the planetary floating member drives the unit 2, this is a favorable, non-regenerative zone, the power flow is shown in Figure 3.7. From the lockup ratio on, the planetary floating member is driven by unit 2, this is a regenerative zone of power circulation, the power flow is shown in Figure 3.8.

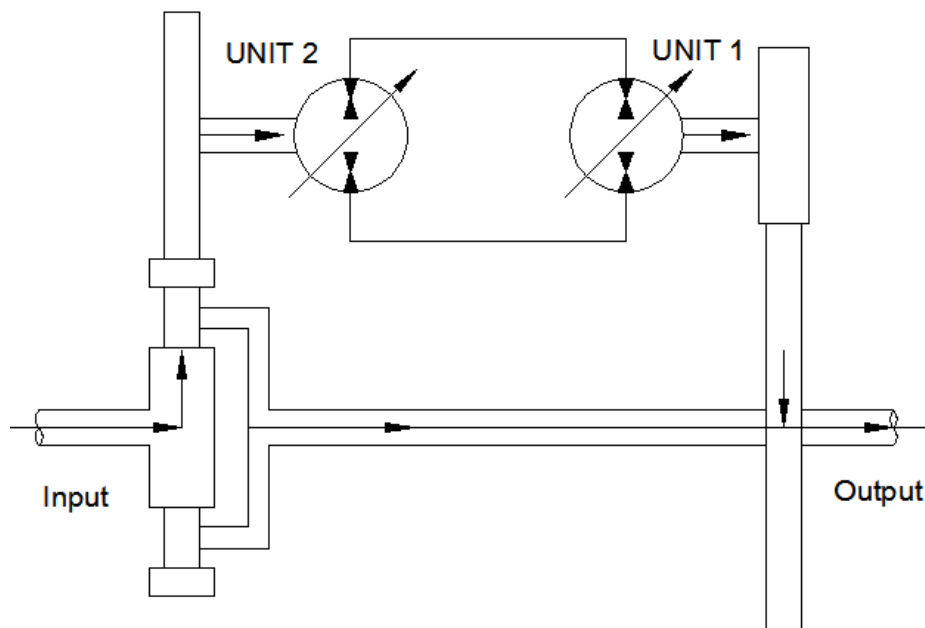


**Figure 3.7** Non-regenerative of output coupled

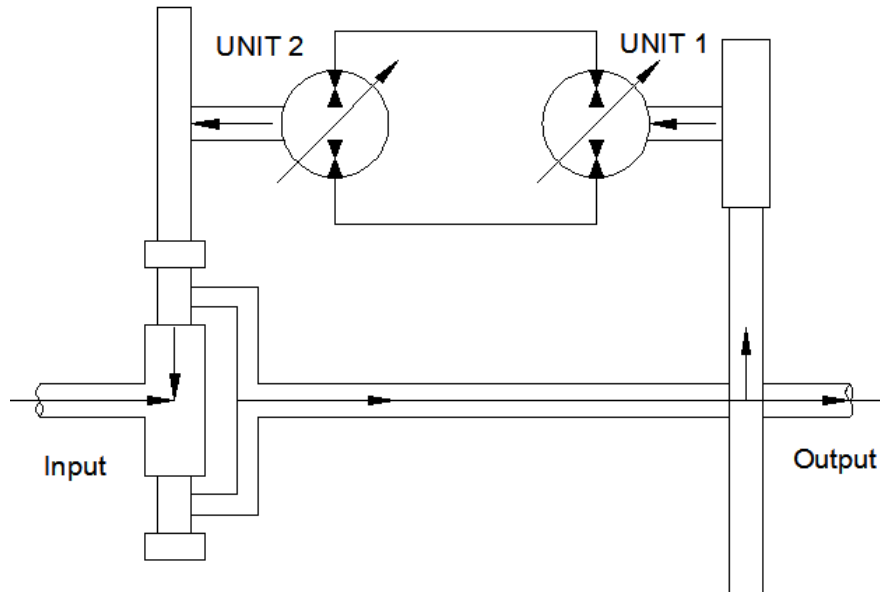


**Figure 3.8** Regenerative of output coupled circuit

The possible power flow of the output coupled circuit system is shown in the following figures.

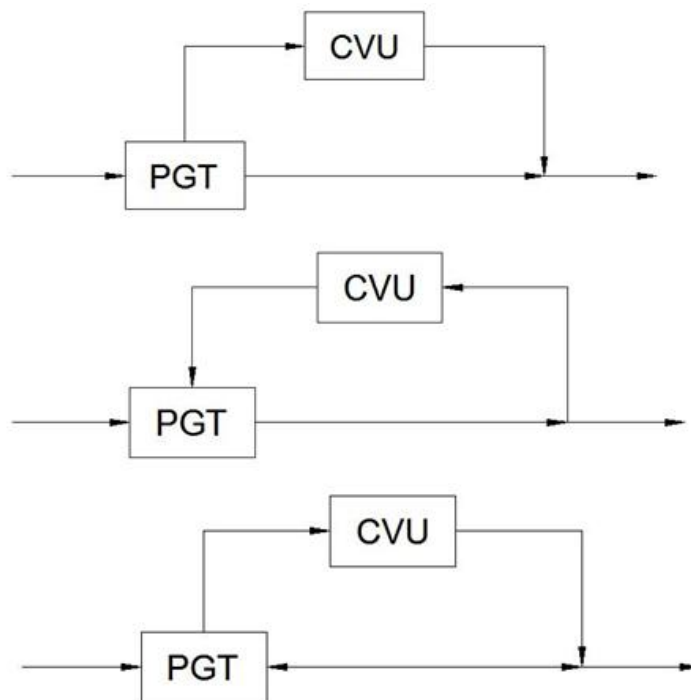


**Figure 3.9** Possible power flow of output coupled

The theoretical percentage of entry power that enters in the hydraulic path is expressed as a function of the transmission ratio

$$P_h = 1 - \frac{R_t}{R_{tl}} \quad (19)$$

As a result the power enters in the mechanical path is

$$P_m = 1 - P_h \quad (20)$$

### 3.2.2 Power distribution diagram

Similarly to the input coupled circuit it is possible to determine the type of the transmission: Non-regenerative (NR), Mechanical regenerative (MR), and Variable unit regenerative (VR).

**Table 3.2** Transmission ratio and transmission type of Output coupled circuit

Transmission ratio $R_t$	Transmission type	Hydraulic power portion $P_h$
$R_t < 0$	VR	$P_h > 1$
$0 < R_t < R_{tl}$	NR	$0 < P_h < 1$
$R_t > R_{tl}$	MR	$P_h < 0$

Here are the explanations of the parameters:

- Transmission ratio in the mechanical path of the planetary gear train  $R_t$
- Transmission ratio at the lockup point  $R_{tl}$
- The power portion in the hydrostatic path  $P_h$
- The power portion in the mechanical path  $P_m$

$$P_h = \frac{R_t}{R_{tl}} \quad (21)$$

$$P_m = 1 - \frac{R_t}{R_{tl}} \quad (22)$$

Based on the formula the power distribution diagram is expressed as:

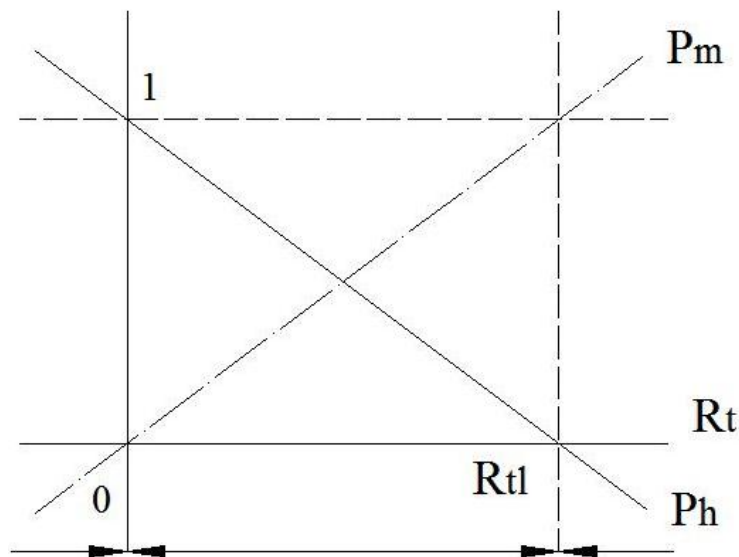


**Figure 3.10** Power distribution diagram of output coupled

### 3.2.3 Output coupled model

In output coupled configuration as shown in Figure 3.11, the engine drives the sun gear of the planetary and the ring gear of the planetary drives the hydraulic pump. The hydraulic motor adds torque to the output shaft. The speed of the engine is divided into two parts, and transmitted via hydrostatic path and mechanical path. The torque of the output shaft is the speed summation of the two paths.

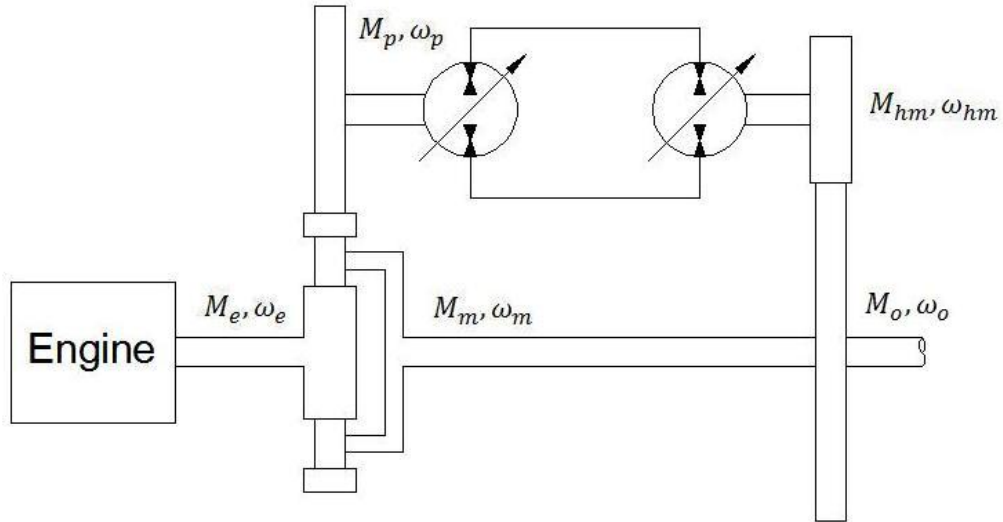


**Figure 3.11** Input coupled model

In the beginning of the operation, the engine side hydrostatic unit is at zero displacement, while the output side hydrostatic unit is at the maximum displacement, the power at this point is transmitted totally by mechanical path. Then the engine side hydrostatic unit displacement increases in the positive direction, as a result the ratio of the hydrostatic transmission is increased, the output speed is increased as well, the hydraulically transmitted power is added to the mechanically transmitted power.

When the engine side hydrostatic unit displacement is decreased in the negative direction, the hydrostatic path circuits a part of power back to the it. At the zero output speed operating point, the mechanically transmitted power is totally circuited. This is an unfavorable situation, the design of the transmission should avoid this situation.

According to Mikko Erkkilä (2009) the parameters of the input coupled circuit are defined as:

- $\omega_e$  and  $M_e$  are the angular velocity and torque of the engine,
- $\omega_p$  and  $M_p$  are the angular velocity and torque of the pump,
- $\omega_{hm}$  and  $M_{hm}$  are the angular velocity and torque of the hydraulic motor,
- $\omega_m$  and  $M_m$  are the angular velocity and torque of the mechanical path,
- $\omega_o$  and  $M_o$  are the angular velocity and torque of the output shaft,
- $\omega_c$  is the angular velocity of the ring gear of the planetary.

The coefficients of the output coupled circuit are determined as follows:

$$k_1 = \omega_c / \omega_e \quad (23)$$

$$k_2 = \omega_c / \omega_m \quad (24)$$

$$k_3 = \omega_p / \omega_c \quad (25)$$

$$k_4 = \omega_o / \omega_{hm} \quad (26)$$

Based on the coefficients the diagram of output coupled circuit can be drawn like Figure 3.12:

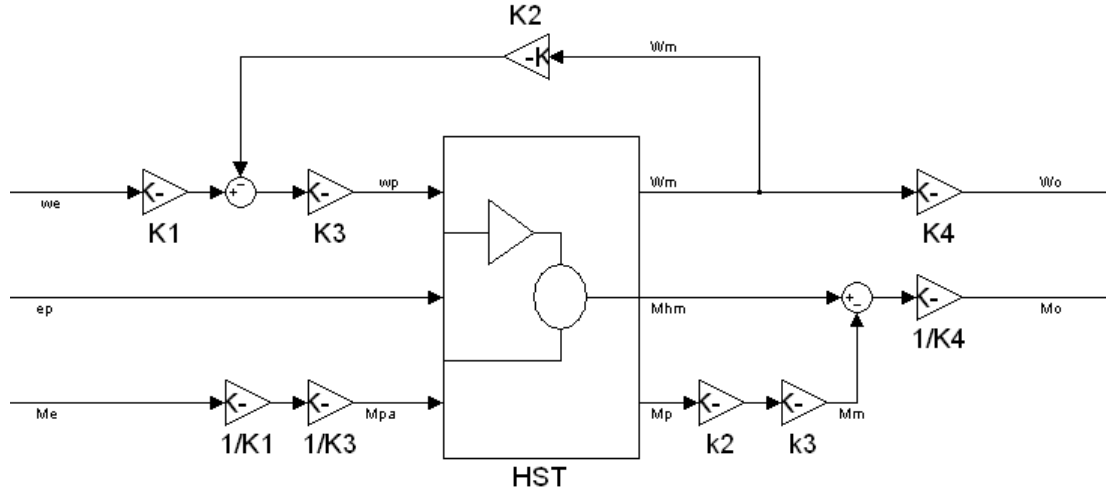


**Figure 3.12** Input coupled block diagram

The pump torque and speed are

$$\omega_p = k_k \varepsilon_p (k_1 \omega_e - k_2 \omega_{hm}) \quad (27)$$

$$M_{pa} = \frac{M_e}{k_1 k_2} \quad (28)$$

The output speed and torque are

$$\omega_o = k_4 \omega_{hm} \quad (29)$$

$$M_o = \frac{1}{k_4} (M_{hm} + k_2 k_3 M_p) \quad (30)$$

Here

$M_{pa}$  is the available torque to the input of pump

$M_p$  is the actual pump torque

By determining general speed ratios

$$k_p = \omega_p / \omega_e \quad (31)$$

$$k_{mp} = \omega_p / \omega_o \quad (32)$$

$$k_{hm} = \omega_o / \omega_{hm} \quad (33)$$

The pump speed and torque are

$$\omega_p = k_p \omega_e - k_{mp} \omega_o \quad (34)$$

$$M_{pa} = M_e / k_p \quad (35)$$

The output speed and torque are

$$\omega_o = k_{hm} \omega_{hm} \quad (36)$$



$$M_o = \frac{M_{hm}}{k_{hm}} + \frac{M_p}{k_{mp}} \quad (37)$$

### 3.3 The variable bridge transmission

The variable CVT shown in Figure 3.13 is a combination of the speed and torque summation systems with at least two planetary gears. Since the bridge design leads to a complicated mechanical design that offers no major advantages over the basic designs, it is not widely used (Mikko Erkkilä 2009). Figure shows the basic idea of the variable bridge transmission.

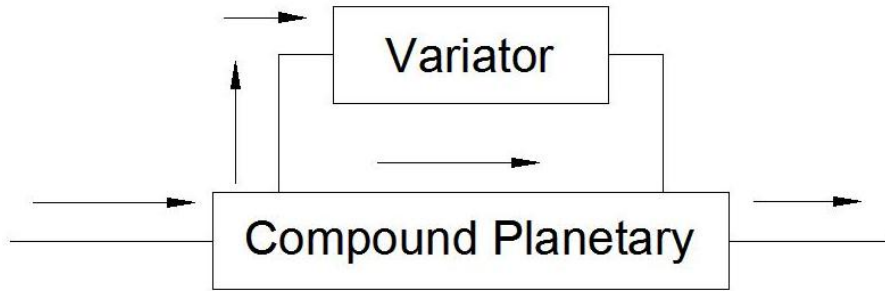


**Figure 3.13** Variable bridge transmission

### 3.4 Steady state hydrostatic transmission models

The hydrostatic transmission circuit plays an important in hydrostatic-mechanical power split CVT, it acts as the continuous variable unit to alter the output speed and the torque. The outputs of the hydrostatic transmission are the output torque  $M_{hm}$  and the output angular velocity  $\omega_{hm}$  of the hydraulic motor for given pump and motor displacement  $V_p$  and  $V_m$ , input torque  $M_{pa}$  and input angular velocity  $\omega_p$ , pump and motor displacement setting  $\varepsilon_p$  and  $\varepsilon_m$ . The pump and motor models were based on the theory of Thoma (1964).

#### 3.4.1 Pump model

The pump model calculates the pump torque and flow for given pump displacement  $V_p$ , input angular velocity  $\omega_p$ , pressure difference  $\Delta P$ , and the displacement setting  $\varepsilon_p$ . The Simulink model can be found in Appendix A.

1) Pump flow

$$Q_p = \frac{\varepsilon_p V_p \omega_p}{2\pi} - Q_{lp} \quad (38)$$

Here  $Q_{lp}$  is the leakage flow of the pump, and it is defined as

$$Q_{lp} = f(\varepsilon_p, \omega_p, \Delta P) \quad (39)$$

2) Pump torque

$$M_p = \frac{\varepsilon_p V_p \Delta P}{2\pi} + M_{lp} \quad (40)$$

$M_{lp}$  is the hydro-mechanical torque loss of the pump, defined as

$$M_{lp} = f(\varepsilon_p, \omega_p, \Delta P) \quad (41)$$

### 3.4.2 Motor model

The motor model calculates the motor torque and flow for the given displacement  $V_m$ , the motor speed  $\omega_m$ , the pressure difference  $\Delta P$ , and the displacement setting  $\varepsilon_m$ . The Simulink model can be found in Appendix B.

1) Motor flow

$$Q_{hm} = \frac{\varepsilon_m V_m \omega_m}{2\pi} + Q_{lm} \quad (42)$$

$Q_{lm}$  is the leakage flow of the motor, and it is defined as

$$Q_{lm} = f(\varepsilon_m, \omega_m, \Delta P) \quad (43)$$

2) The motor torque is

$$M_{hm} = \frac{\varepsilon_m V_m \Delta P}{2\pi} - M_{lhm} \quad (44)$$

$M_{lhm}$  is the hydro-mechanical torque loss of the motor, defined as

$$M_{lhm} = f(\varepsilon_m, \omega_m, \Delta P) \quad (45)$$

### 3.5 Summary

This chapter introduced the basic hydrostatic-mechanical power split CVT circuits, studied the power flow of the circuits, and modeled the circuits. For the input-coupled circuit, the power flows in different paths are

$$P_h = 1 - \frac{R_{tl}}{R_t} \quad (46)$$

$$P_m = \frac{R_{tl}}{R_t} \quad (47)$$

The pump speed and torque are

$$\omega_p = k_p \omega_e \quad (48)$$

$$M_{pa} = \frac{1}{k_p} \left( M_e - \frac{M_o}{k_m} \right) \quad (49)$$

The output speed and torque are

$$\omega_o = k_{hm} \omega_{hm} + k_m \omega_e \quad (50)$$

$$M_o = \frac{M_{hm}}{k_{hm}} \quad (51)$$

For the output-coupled circuit, the power flows in different paths are

$$P_h = \frac{R_t}{R_{tl}} \quad (52)$$

$$P_m = 1 - \frac{R_t}{R_{tl}} \quad (53)$$

The pump speed and torque are

$$\omega_p = k_p \omega_e - k_{mp} \omega_o \quad (54)$$

$$M_{pa} = M_e / k_p \quad (55)$$

The output speed and torque are

$$\omega_o = k_{hm} \omega_{hm} \quad (56)$$

$$M_o = \frac{M_{hm}}{k_{hm}} + \frac{M_p}{k_{mp}} \quad (57)$$

## 4 Steady State Characteristics

The steady state characteristics investigation on the mathematical models of input and output coupled circuits of hydrostatic-mechanical power split CVT demonstrates the velocity response of the different configurations to the control signal, and the power distribution curve during the control process.

### 4.1 Input coupled speed summation

The schematic is shown in Figure 4.1, the simulink model can be found in Appendix C.

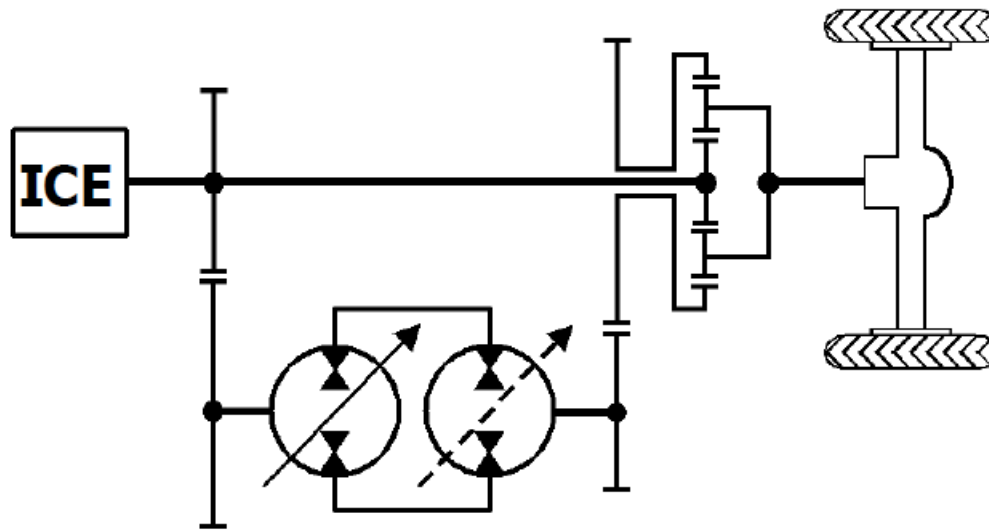


**Figure 4.1** Input coupled driveline schematic (Ivantysynova Monika 2010)

1) The simulation parameters

**Table 4.1** Input coupled driveline simulation parameters

Engine Power	$P_e = 100 \text{ kW}$
Engine angular velocity	$\omega_e = 209.4 \text{ rad/s} = 2000 \text{ rpm}$
Speed ratio between engine and pump	$K_p = 1$
Speed ratio between output shaft and pump	$K_{mp} = 0.5$
Speed ratio between output shaft and motor	$K_{hm} = 0.5$
Pump displacement	$V_p = 100 \text{ cm}^3/\text{rev}$
Motor displacement	$V_m = 200 \text{ cm}^3/\text{rev}$
Speed ratio between output shaft and drive wheel	$i_{FR} = 36.5$
Drive wheel radius	$r = 905 \text{ mm}$

The traction effort  $F_t$  and the velocity  $V$  were as

$$F_t = i_{FR} M_o / r \quad (58)$$

$$V = \frac{\omega_o r}{i_{FR}} \quad (59)$$

The mechanically transmitted power  $P_m$ , hydraulically transmitted power  $P_h$ , output power  $P_o$  and  $P_i$  were calculated as follows

$$P_m = k_m \omega_e M_o \quad (60)$$

$$P_h = \Delta P Q \quad (61)$$

$$P_o = \omega_o M_o \quad (62)$$

$$P_i = k_p M_p + k_m M_o \quad (63)$$

The overall efficiency is

$$\eta = \frac{P_o}{P_i} \quad (64)$$

## 2) The pump and motor displacement settings

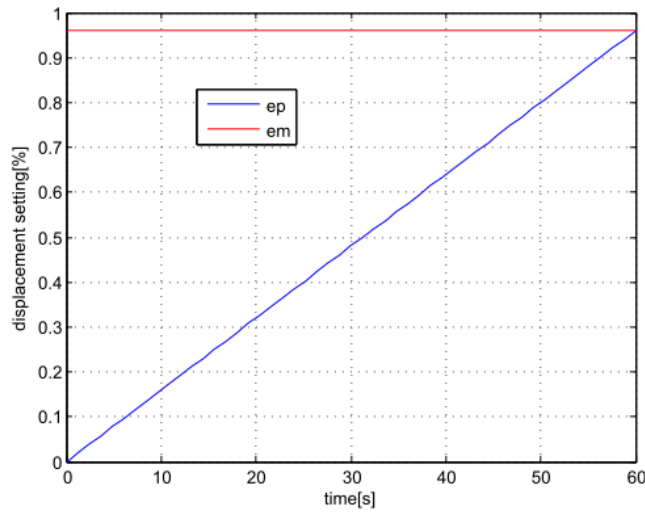


**Figure 4.2** Pump and motor displacement setting

As shown in the Figure 4.2, in the beginning of the simulation the pump is at zero displacement and the motor is at the maximum displacement. During the the simulation the pump displacement setting  $\varepsilon_p$  increase from 0 to 1, while the motor displacement setting  $\varepsilon_m$  keeps constant at 1.

## 3) The simulation results

In most cases, the gear ratios are selected such that minimum speed is zero output speed and the transmission is only in one direction, reverse is realized by using a power shuttle.

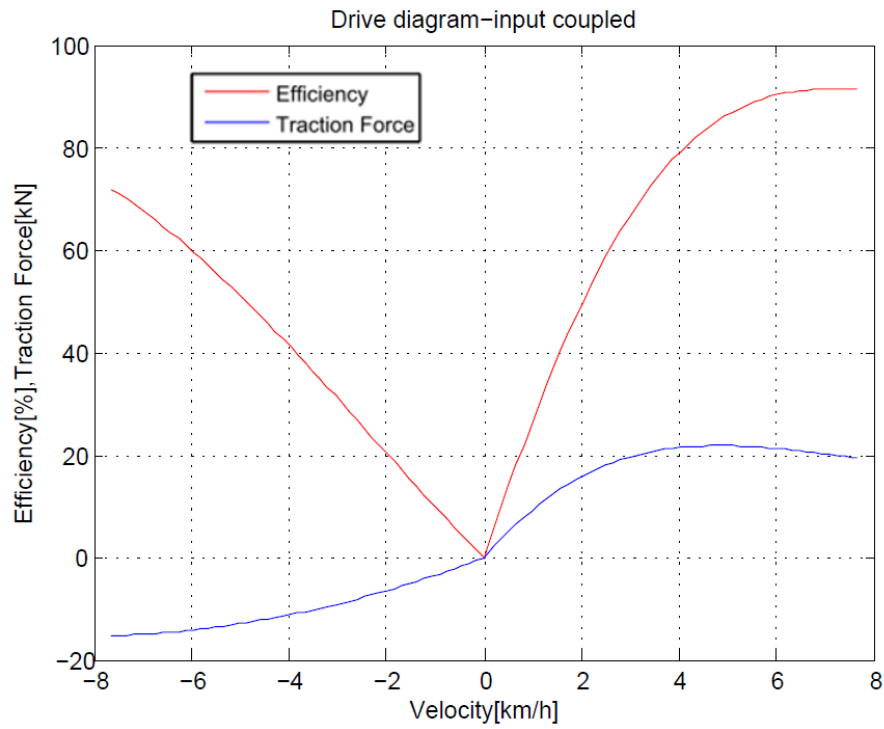


**Figure 4.3** Input coupled drive diagram

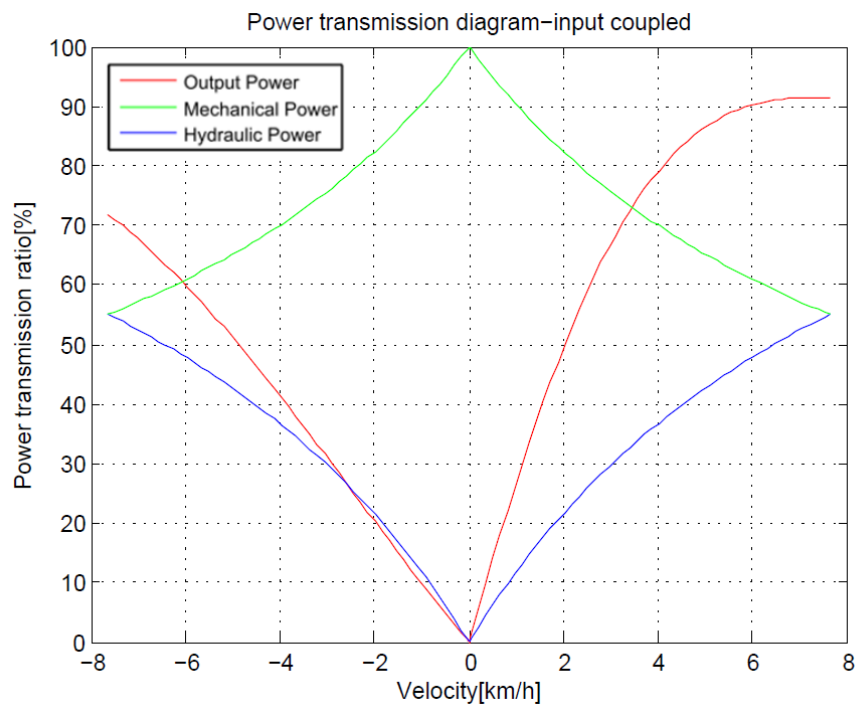


**Figure 4.4** Input coupled power transmission diagram

The traction force is influenced by the portion of the hydrostatic transmission, the higher the portion of the hydrostatic transmission, the larger the traction force is. In practical applications additional gear trains are used to increase the output speed.

## 4.2 Output coupled simulation

The scheme is as Figure 4.5, the simulink model can be found in Appendix D:

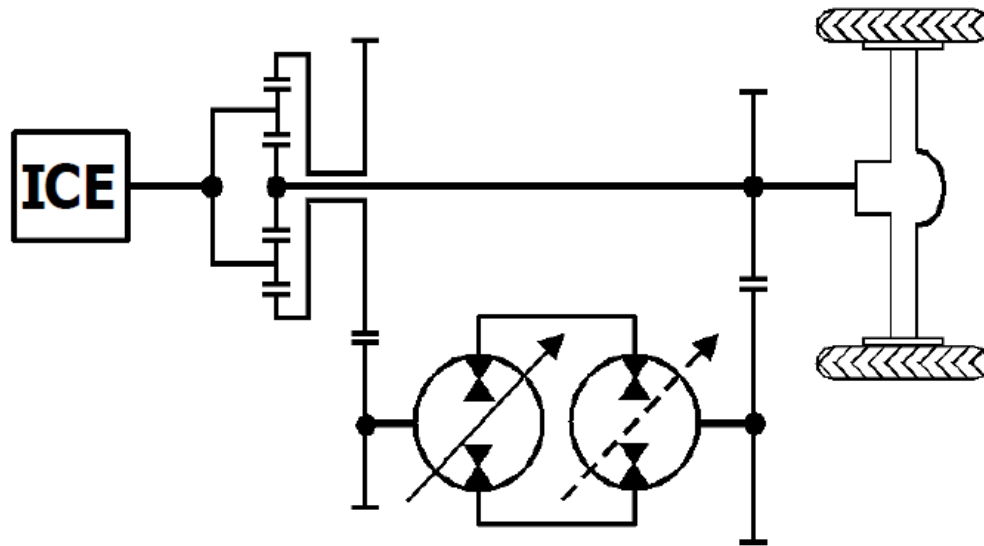


**Figure 4.5** Output coupled driveline (Ivantysynova Monika 2010)

### 1) Simulation parameters

**Table 4.2** Output coupled simulation parameters

Engine Power	$P_e = 100 \text{ kW}$
Engine angular velocity	$\omega_e = 209.4 \text{ rad/s} = 2000 \text{ rpm}$
Speed ratio between engine and pump	$K_p = 1$
Speed ratio between output shaft and pump	$K_{mp} = 1$
Speed ratio between output shaft and motor	$K_{hm} = 1$
Pump displacement	$V_p = 100 \text{ cm}^3/\text{rev}$
Motor displacement	$V_m = 200 \text{ cm}^3/\text{rev}$
Speed ratio between output shaft and drive wheel	$i_{FR} = 36.5$
Drive wheel radius	$R = 905 \text{ mm}$

### 2) The pump and motor displacement settings

At the starting point, the motor is in the maximum displacement, while the pump is in zero displacement. Then the pump displacement keep increase to the maximum displacement, after that the motor displacement decrease to zero.

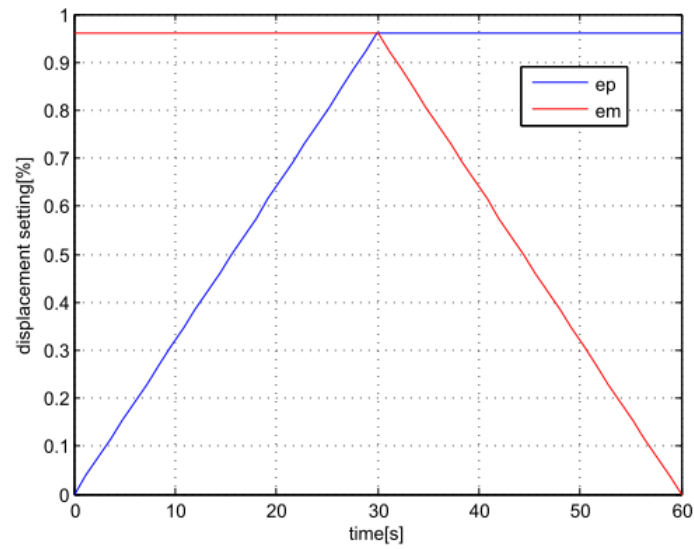


**Figure 4.6** Pump and motor displacement settings

### 3) The simulation results

The overall efficiency can reach more than 90%, which is very promising for practical applications.

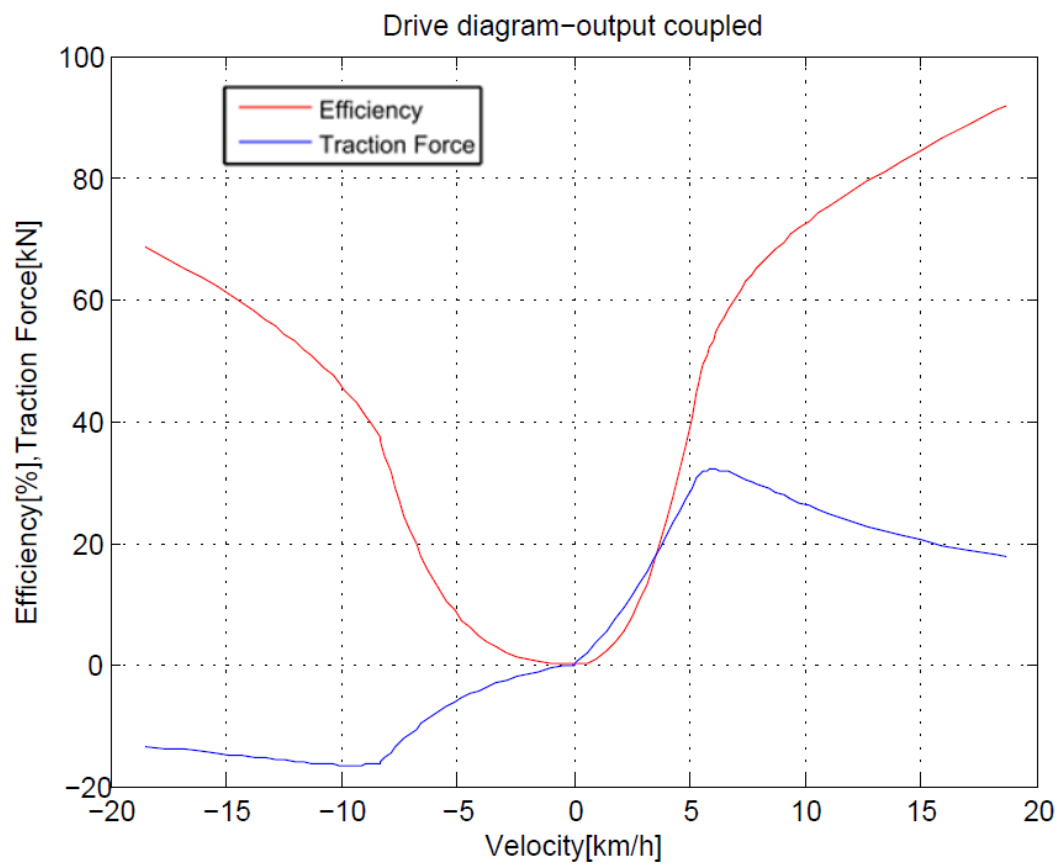


**Figure 4.7** Drive diagram of output coupled driveline



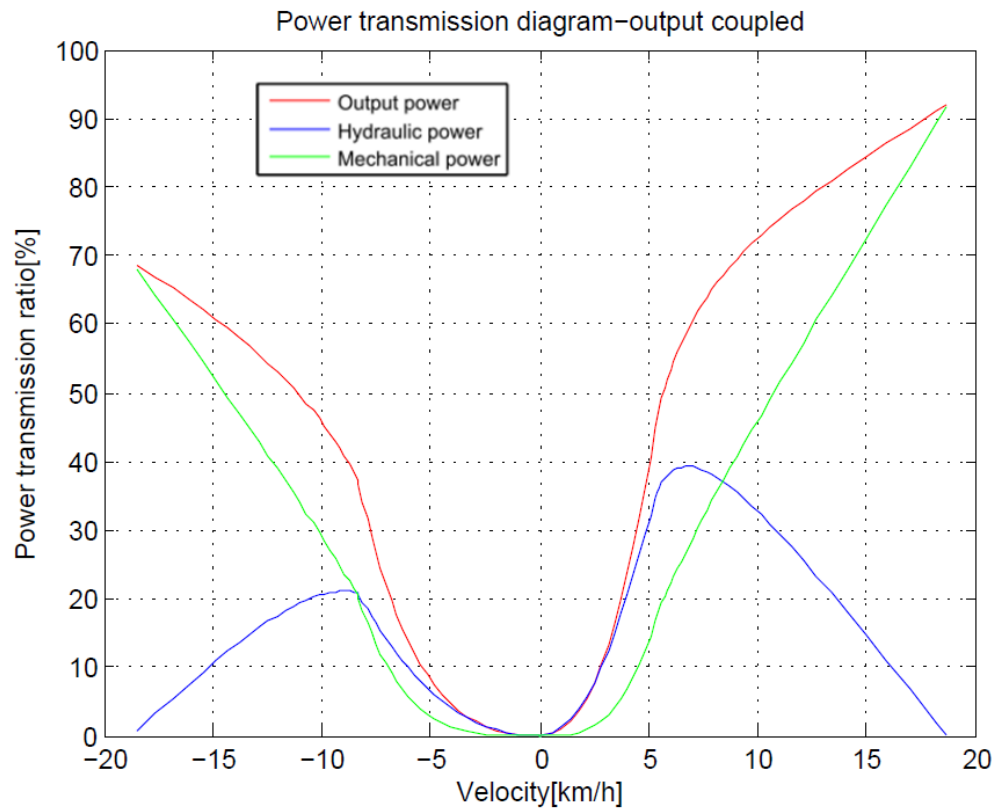


**Figure 4.8** Power transmission diagram of output driveline

Figure 4.7 shows the drive diagram of the output coupled circuit, and Figure 4.8 shows the power distribution diagram of the output coupled circuit. Hydrostatic power portion is 100 % in the starting point, but zero at the top speeds of the ranges. It can be seen from the diagrams that with the decrease of the portion of hydrostatic transmission, the overall efficiency keeps increasing, however the traction force decrease too, so the portion of hydrostatic transmission should be controlled according to the actual situation. In practical applications additional gear trains are used to increase the output speed.

### 4.3 Summary

This chapter studied the steady-state characteristics of input and output coupled circuits, the simulation results show that both the advantages and disadvantages of input and output coupled circuits. Input coupled circuits are mainly used in one direction drive. The main advantage of input coupled circuit is its simplicity to be propagated to multi stage transmissions. The main advantages of output coupled circuits are the good transmission property in both drive direction, and the good efficiency it offers in a wide range of transmission rate.

The lockup point is the point at which a power split CVT transmission becomes purely mechanical, with the ring gear being stationary. The transmission ratio in this situation is known as the lockup ratio. When designing a power split CVT transmission, the first step is to analyze the planetary gear train to achieve the lockup ratio, once the lockup ratio is known the whole transmission ratio can be calculated using it. The benefits of the lockup point should be considered in practical engineering application, this point is favorable for heavy duty working speed. Once the lockup point ratio is known, the power distribution at any given time can be determined.

## 5 HMPS-CVT Application

In the era of increasing fuel economy and reducing environment pollution, the development of vehicle with new environment friendly and high efficient proposition system becomes a necessity. Hybrid vehicles are one of the means to realize the goal. This chapter reviews the current application of hydrostatic-mechanical power split CVT in working machines, to provide information of the ways how the concept of basic circuits of hydrostatic-mechanical power split CVT configure into real system and their corresponding performance.

### 5.1 The Claas-Jarchow HM-8 and HM-II

Claas carried out a great amount of pioneering works since the late 1980s, which resulting in the concepts Claas HM-8 (about 140 kW) and the later larger Claas HM-II, also known as Traxion (about 220 kW). Both of the concepts were based on a patent of Jarchow (Jarchow 1981), and they have been developed for the Claas carrier tractor Xerion. The HM-8 had 7 power split ranges so that to keep the hydrostatic power portion low and efficiency high. One creeper range works direct. The resulting tractors was produced since 1996, while the HM-II (Traxion) with 5 power split ranges, one direct and a conventional power shift reverser by clutches was presented at Agritechnica 1999 (Renius, K. Th., Resch, R. 2005). Both types were produced at limited production volume. The Claas-Jarchow approach is characterized by an input coupled four-shaft compound planetary which consists of two standard planetaries (Jarchow 1981). The shifts between the ranges are done at synchronous speeds with dog clutches and the power is handed over without any power interruption in a very short time, in which the ratio is kept constant (no acceleration/deceleration of the vehicle). This principle is very difficult to realize but does not need friction clutches (reduced costs, idling, losses). However, a high sophisticated electronic control system is required. The measured Claas HM-8 efficiencies have been found to be quite good which can cover the target of the diagram.

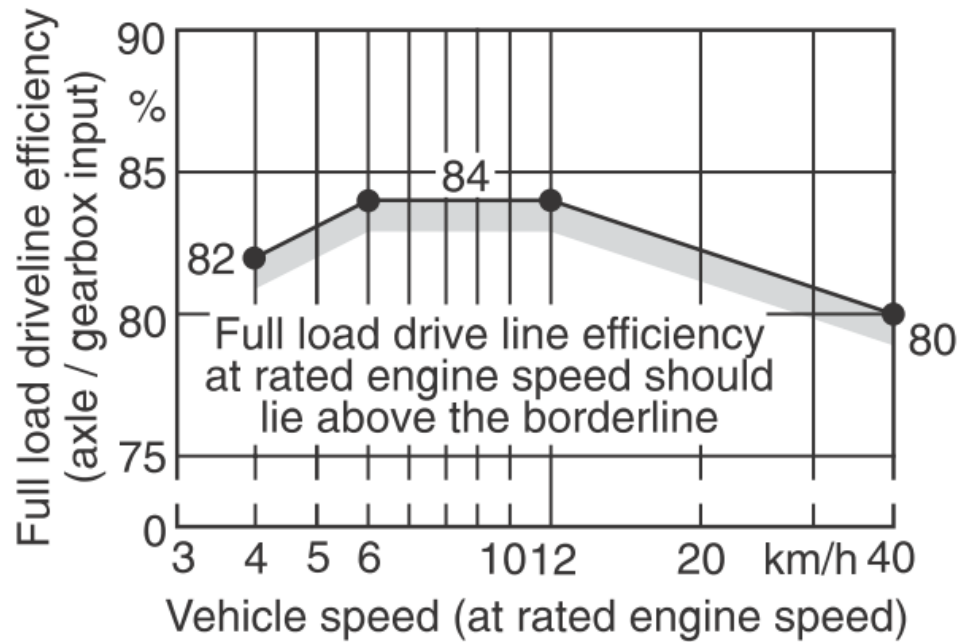


**Figure 5.1** Efficiency target for CVT of larger tractors above 100kW (Renius 1999)

## 5.2 The Fendt Vario

Fendt equipped the Fendt tractor 926 Vario (191 kW) with its new, infinitely variable Vario transmission at Agritechnica 1995. The scheme is shown in Fig. 5.2. It became the worldwide first in series produced power split transmission for standard tractors (1996). Its principle was soon expanded to more and more other Fendt models families. At the end of 2004 four tractor families 400, 700, 800 and 900 were in production with the Vario CVT as standard transmission.

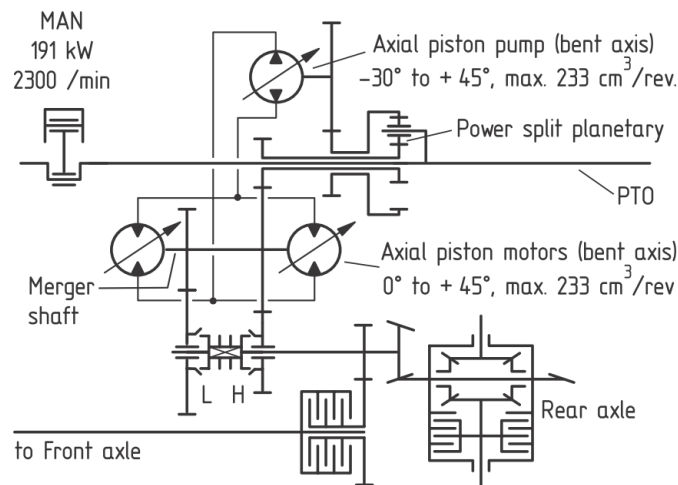


**Figure 5.2** Fendt Vario for the tractor Favorit (1996)

The Fendt Vario is output-coupled power split CVT. The structure is based on a principle of Molly (Renius, K. Th. and Resch, R. 2005). Basic development had been done by the Fendt engineer H. Marschall (Marschall, H. 1973), who got several patents

on it. In the forward direction, power is split by the planetary gear transmission and merged by the shaft of the two hydrostatic units (Dziuba and Honzek 1997). The basic power characteristics follow Fig. 5.3 and 5.4. Hydrostatic power portion is 100 % in the starting point, but zero at the top speeds of the ranges.

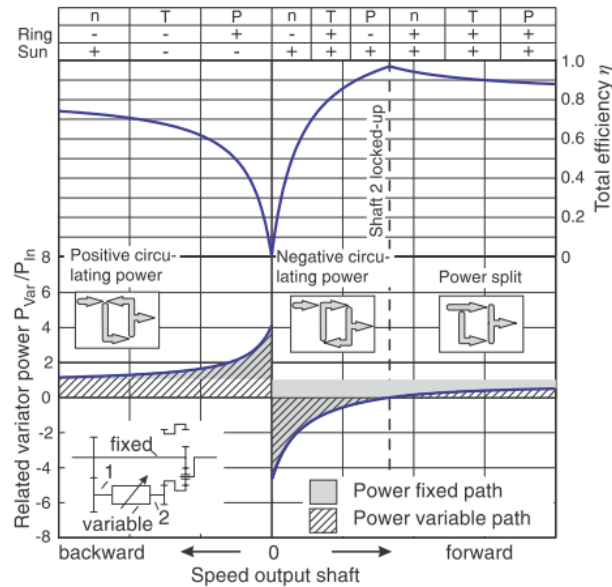


**Figure 5.3** Transmission characteristics of input coupled (Renius, K. Th. and Resch, R. 2005)

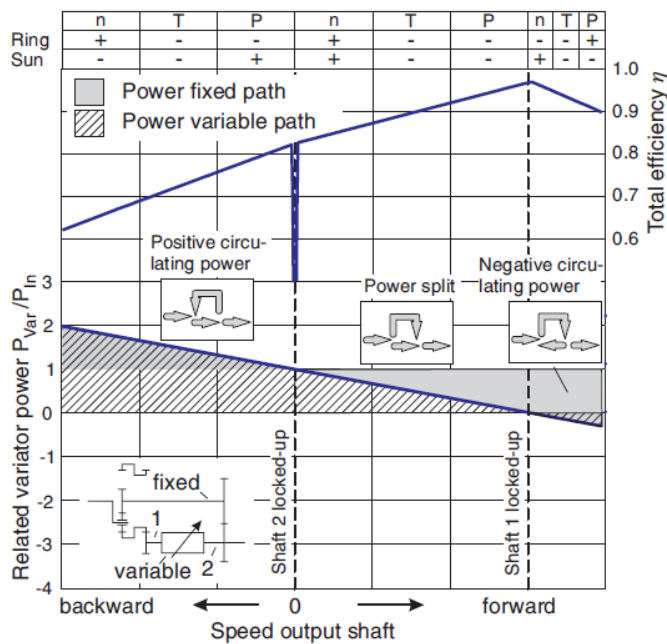


**Figure 5.4** Transmission characteristics (Renius, K. Th. and Resch, R. 2005)

The power split unit covers two ranges: range L, which covers speeds up to 32 km/h, and range H which up to 50 km/h. The top speeds are nears the lock-up points. The speed range beyond the lock-up range is not used to avoid power circulating, thus there is no reversed hydrostatic power. An automatic shift on-the-go was introduced to allow finger tip range selection within a speed band up to 20 km/h. The shift is done by active synchronization support of the CVT. This is quite useful for heavy transports on

hilly roads. The power interruption is quite small that mostly not realized by the driver. For light duty transports, range H is sufficient for all speeds from zero to 50 km/h.

The required maximum hydrostatic power for the Fendt concept is very high, which results in large units. Because commercially available variable axial piston pumps and motors could not meet the efficiency requirements as shown in Figure 5.1, Fendt developed its own 45 degree variable bent axis units, which offer in their best points efficiencies of 95-96 % (swash plate units rather 89-92 %). A serious problem of the Fendt concept was the high noise level due to the large units.

### 5.3 The Steyr S-Matic for Steyr, Case, New Holland

The Steyr S-Matic had been developed within the 1990s by the Austrian company Steyr Antriebstechnik (SAT) which was later taken over by Zahnradfabrik Passau GmbH in 2000. The first concept became public in 1994, and series production was announced with a modified structure (Zbigniew Żebrowski 2007) and realized early 2000 for the standard tractors Steyr CVT and the Case CVX (both 88-125 kW). The transmission was also adopted by New Holland TVT tractor series (2004), and McCormick introduced it to a new tractor series VTX in 2005/2006.

The S-Matic is an input coupled type power split CVT with a five shaft compound planetary, which consists of two standard planetaries and a planetary for reverse, the configuration is shown in the Figure 5.5.

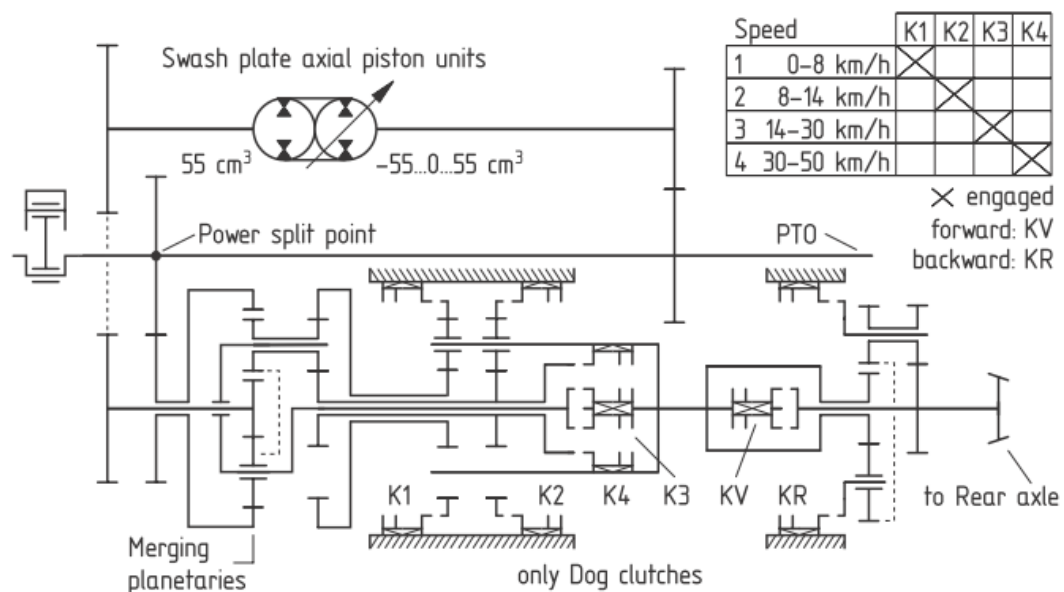


**Figure 5.5** The S-Matic hydrostatic power split CVT (Zbigniew Żebrowski 2007)

Four ranges vary between zero and 50 % are used to keep the hydrostatic power level low. The ranges are shifted at synchronous speeds using the dog clutches K1, K2, K3 and K4 (Aitzetmüller Heinz 2000). The power is handed over without power interruption. The interruptions of acceleration could be made very short as demonstrated by Fig. 37.

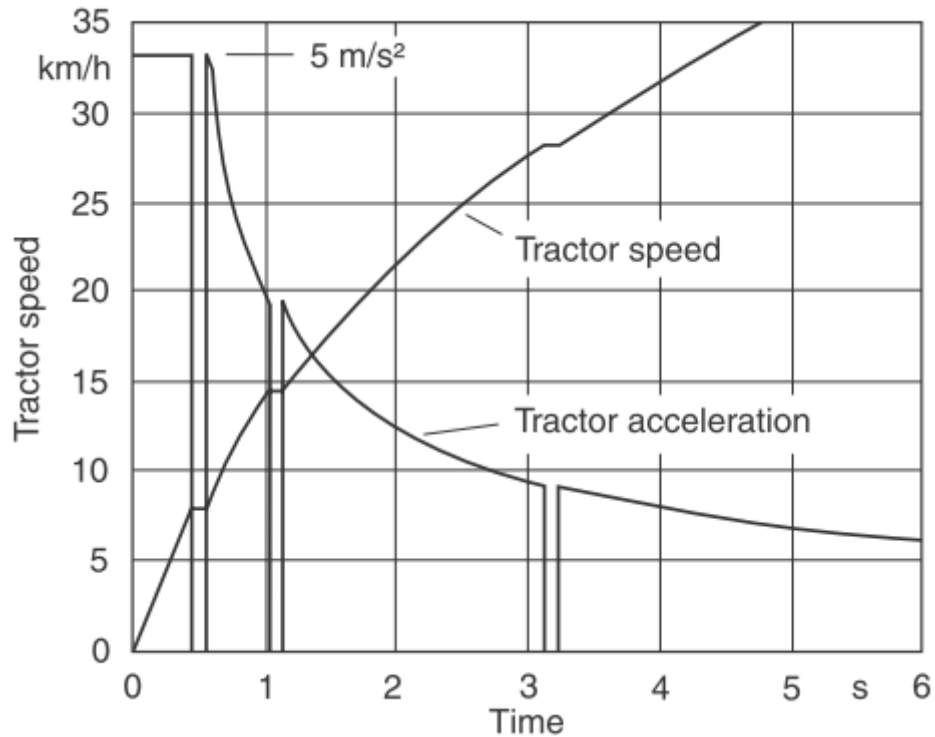


**Figure 5.6** Tractor drive diagram (Zbigniew Żebrowski 2007)

Efficiencies of the S-Matic have been published by Leitner et al. (2000) excluding axles, which is shown in Figure 5.7.

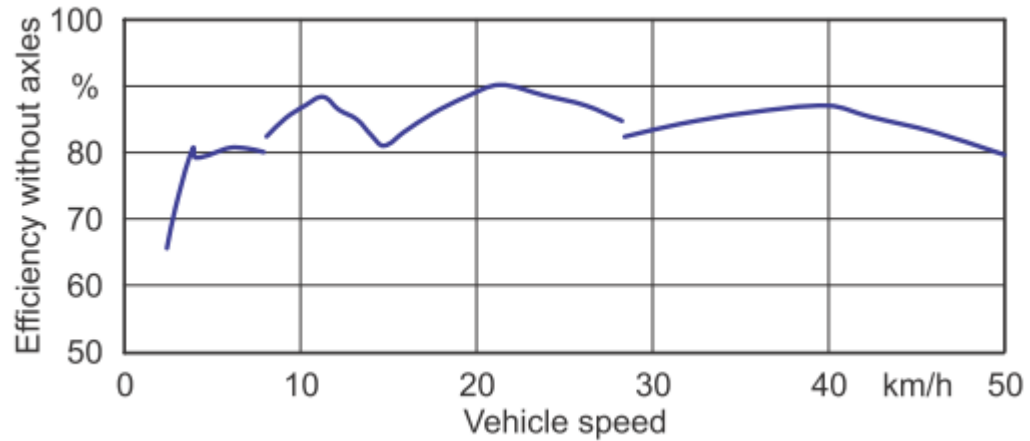


**Figure 5.7** Efficiency diagram (Aitzetmüller Heinz 2000)

#### 5.4 The ZF Eccom for Deutz-Fahr, John Deere, Claas

ZF Eccom was first announced by ZF/ZP at Agritechnica 97. The configuration of ZF Eccom is like:

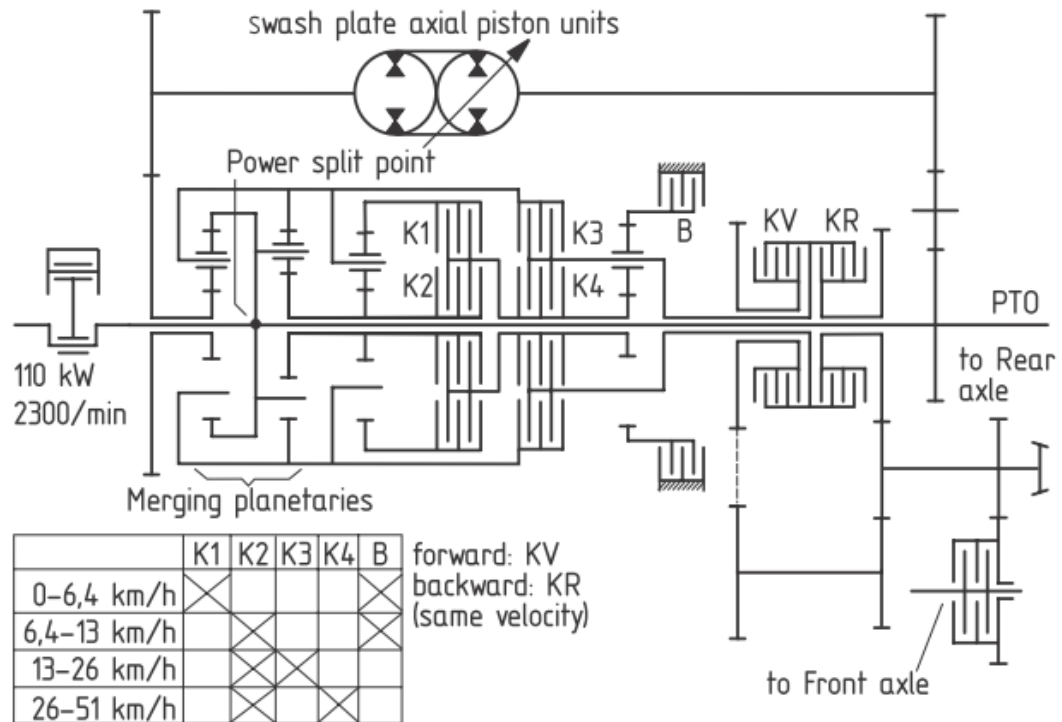


**Figure 5.8** ZF - Eccom hydrostatic-mechanical power split CVT (Zbigniew Żebrowski 2007 )

There are three transmission families within ZF-Eccom: 1) Eccom 1.5 (110kW); 2) Eccom 1.8 (130kW); 3) Eccom 3.0 (220kW). Deutz-Fahr was the first tractor company using the Eccom (version 1.5) in its new series Agrotion TTV (92/103/110 kW). John Deere applies the Eccom since 2001 for its 6000 tractor line known as AutoPower. Claas has announced to use the Eccom 3.0 for its new Xerion carrier tractor family.

The concept of the power split system is a type of input coupled circuit. The four ranges concept keeps the hydrostatic power in a low level. Figure below illustrates the linear output speed variation of the hydrostatic unit between minus 2300 and plus 2300 rpm crossing at zero the lockup point (Zbigniew Żebrowski 2007).



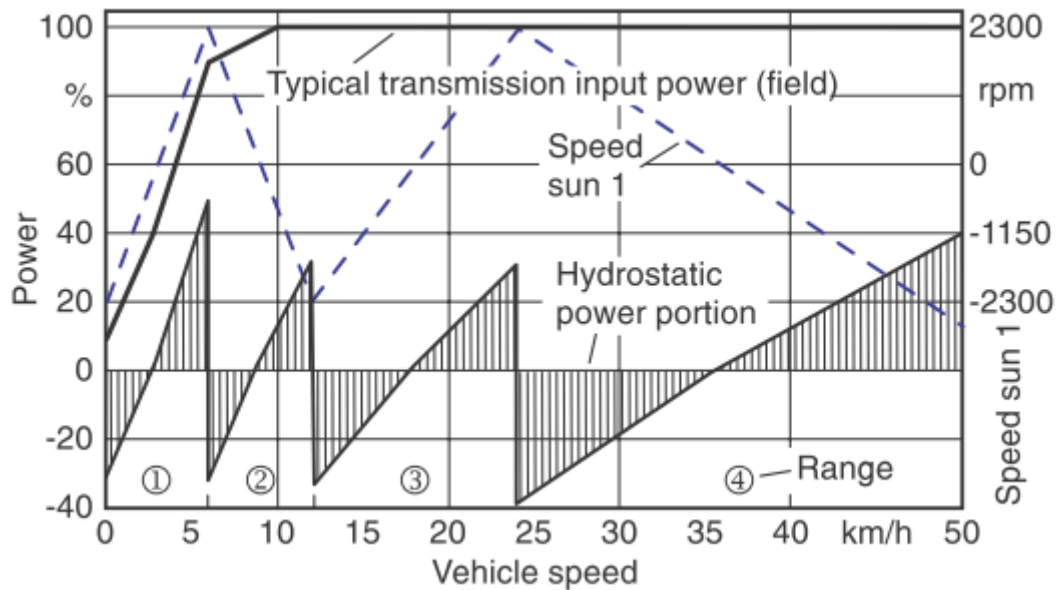


**Figure 5.9** Hydrostatic power portions and speed of first left sun gear within the 4 ranges (Pohlenz and Gruhle 2002)

Two planetaries are used, the first of which is a five-shaft compound planetary that combines three standard planetaries, the second of which is a standard planetary. This compound planetary produces 3 ranges using friction clutches K1, K2 and K3, while the standard planetary produces the fourth range K4. Forward and reverse shift is realized by using two conventional reverser clutches KV, KR. The clutch dimensions are large due to the high possible slipping speeds. Efficiencies of this transmission are published excluding the axles (Renius, K. Th., Resch, R.).

## 5.5 Yanmar CVT

Yanmar Agricultural Equipment Co., Ltd., Japan, produced a self propelled rice transplanter in series since 2002 which applies a power split CVT for the vehicle drive. Figure 5.9 shows the concept of Yanmar CVT.

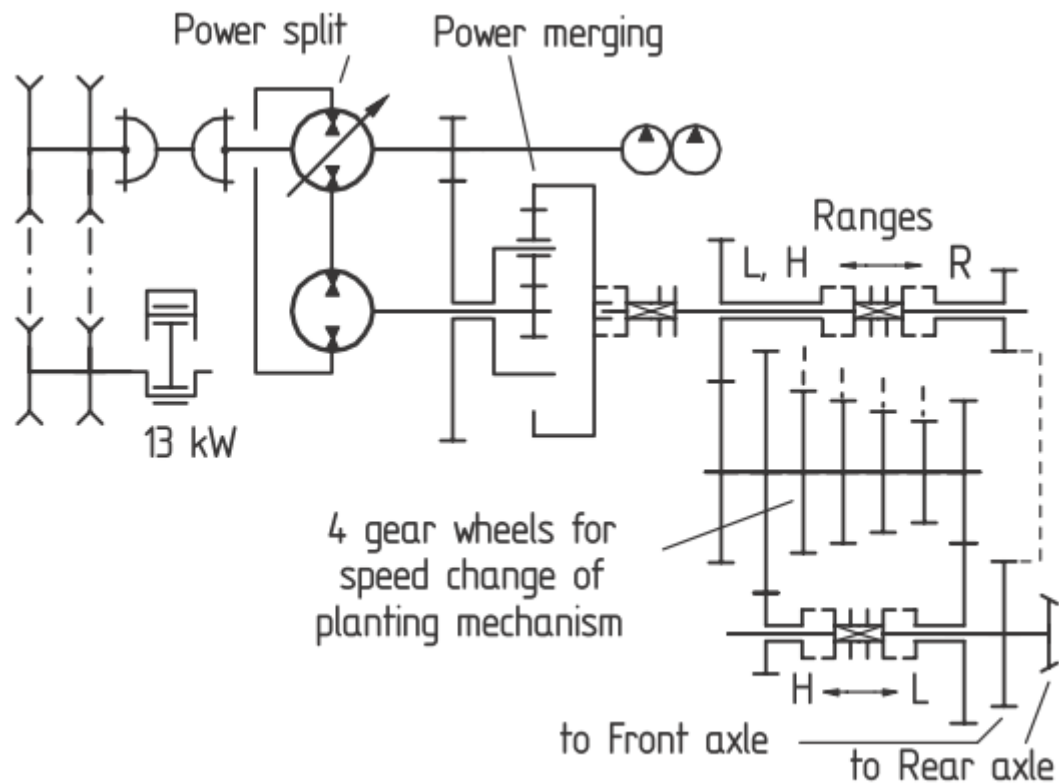


**Figure 5.10** Yanmar CVT (Renius, K. Th., Resch, R 2005)

The 13 kW engine drives both the variable hydrostatic axial piston unit and the carrier of the standard planetary. Power is split within the hydraulic variable unit, while power merging takes place in the planetary with the sun gear connected to the second hydrostatic unit. The concept of the system is input coupled. Power is directed from the planetary ring gear to a conventional gearbox, which contains forward-reverse range, two forward ranges L, H, a speed shift for the planting mechanism and output shafts for rear and front axle. The system has been well accepted by the market according to information from Yanmar (Renius, K. Th., Resch, R 2005).

## 5.6 Summary

The hydrostatic-mechanical power split CVT is a special type of power split CVT, which is suitable for high power density application. The hydrostatic-mechanical power split CVT is not a newly developed technology, Renault (Pablo Noben 2007), derived a famous idea to use the principle of internal hydrostatic-mechanical power split for a passenger car gearbox. The presence of this type of transmission has been increasing ever since its emergence. However, only a handful of mobile machines make use of hydrostatic-mechanical power split CVT. Its potential is far from fully explored. This chapter reviews five concepts of hydrostatic-mechanical power split CVT configurations that commercially developed for larger tractors to give an idea on the practical application of this type of transmission technology and their actual performances, all the concepts demonstrate good properties, four of them could enter series-production stage. Power split CVT provides better system efficiency over the traditional hydrostatic CVT mode, there are great potential markets to be explored in the future.

## 6 Suitability study

This chapter studies the suitability of hydrostatic-mechanical power split CVT technology, the studies include working cycle suitability and power range suitability. The studies aimed to find suitable working conditions for the hydrostatic-mechanical power split CVT, under which it demonstrates good efficiency.

### 6.1 Diesel engine

The diesel engine model made by Daiheng Ni (Daiheng Ni 2008) was used in this study, since this model was proved simple and stable. It makes use of the maximum engine power  $P_{max}$  and maximum engine torque  $T_{max}$  and related angular velocities  $\omega_{pp}$ ,  $\omega_{pt}$ , all these parameters can be found from the specification of an engine. The approximate torque curve is:

$$T = C_1 + C_2(\omega - \omega_{pt})^2 \quad (65)$$

where  $C_1$  and  $C_2$  are constants, and  $\omega_{pt}$  is the engine speed at peak torque. To ensure that the power curve peaks at  $\omega_{pp}$ ,  $C_1$  is replaced with a different coefficient  $C_3$  as:

$$P = C_3\omega + C_2(\omega - \omega_{pt})^2\omega \quad (66)$$

Give that the engine outputs  $P_{max}$  at  $\omega_{pp}$  and output  $T_{max}$  at  $\omega_{pt}$ , the following equations can be derived:

$$T_{max} = C_1 + C_2(\omega_{pt} - \omega_{pt})^2 = C_1 \quad (67)$$

$$P_{max} = C_3\omega_{pp} + C_2(\omega_{pp} - \omega_{pt})^2\omega_{pp} \quad (68)$$

$$\left. \frac{dP}{d\omega} \right|_{\omega=\omega_{pp}} = (C_3 + C_2(\omega - \omega_t)^2 + 2C_2\omega(\omega - \omega_{pt})) \Big|_{\omega=\omega_{pp}} \quad (69)$$

Solve the equations:

$$C_2 = -\frac{P_{max}}{2\omega_{pp}^2(\omega - \omega_{pt})} \quad (70)$$

$$C_3 = \frac{P_{max}}{2\omega_{pp}^2}(3\omega_{pp} - \omega_{pt}) \quad (71)$$

Therefore

$$T = T_{max} - \frac{P_{max}}{2\omega_{pp}^2(\omega_{pp} - \omega_{pt})}(\omega - \omega_{pt})^2 \quad (72)$$

$$P = \frac{P_{max}}{2\omega_{pp}^2}(3\omega_{pp} - \omega_{pt})\omega - \frac{P_{max}}{2\omega_{pp}^2(\omega_{pp} - \omega_{pt})}(\omega - \omega_{pt})^2\omega \quad (73)$$

According to Daiheng Ni the validation curves of the model are shown in Figure 6.1, 6.2, the model used in this study is model two.

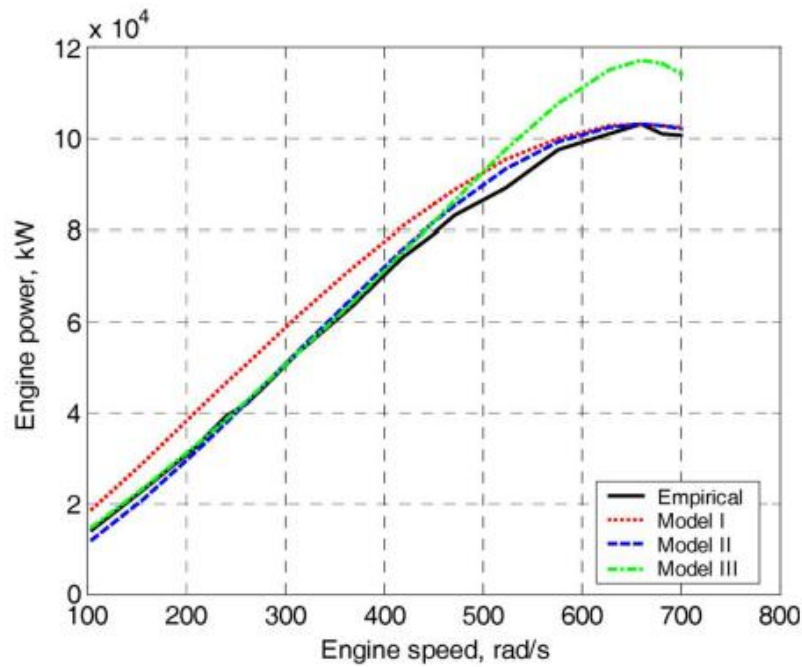


**Figure 6.1** Engine power curve (Daiheng Ni 2008)

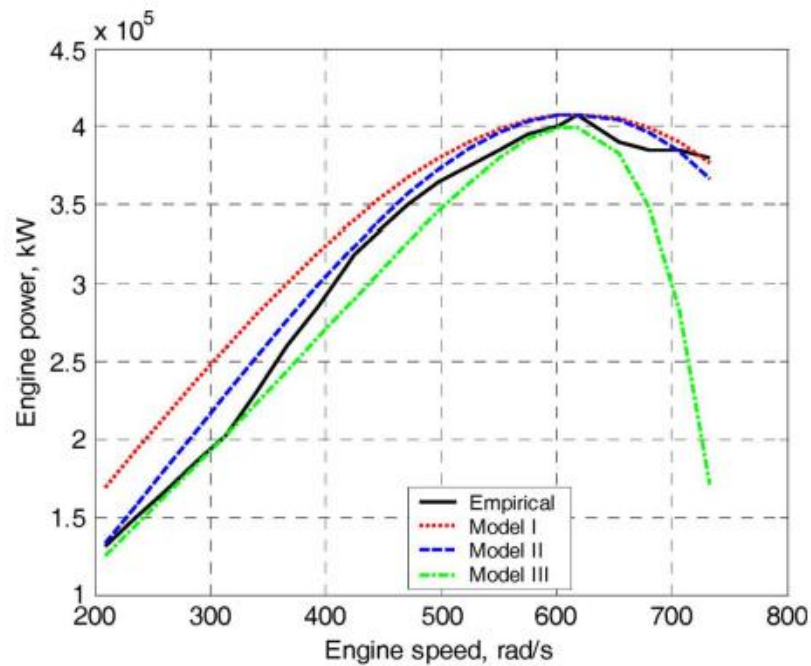


**Figure 6.2** Engine power curve (Daiheng Ni 2008)

## 6.2 Model of hydrostatic transmission

The following assumptions were made for modeling the hydrostatic transmission

- Temperature was assumed to be constant,

- b) Pressure drop and fluid dynamics between pump and motor were ignored,
- c) Low pressure was assumed constant,
- d) No internal or external leakages between pump and motor.

The pump flow is

$$Q_p = \frac{\varepsilon_p V_p \omega_p}{2\pi} - Q_{lp} \quad (74)$$

$Q_{lp}$  is the leakage flow of the pump, and it is defined as

$$Q_{lp} = f(\varepsilon_p, \omega_p, \Delta P) \quad (75)$$

The motor flow is

$$Q_{hm} = \frac{\varepsilon_m V_m \omega_m}{2\pi} + Q_{lm} \quad (76)$$

$Q_{lm}$  is the leakage flow of the motor, and it is defined as

$$Q_{lm} = f(\varepsilon_m, \omega_m, \Delta P) \quad (77)$$

The system continuity equation is

$$\frac{d\Delta P}{dt} = \frac{B(Q_p - Q_{hm})}{V} \quad (78)$$

The motor torque is

$$M_{hm} = \frac{\varepsilon_m V_m \Delta P}{2\pi} - M_{lhm} \quad (79)$$

$M_{lhm}$  is the hydro-mechanical torque loss of the motor, defined as

$$M_{lhm} = f(\varepsilon_m, \omega_m, \Delta P) \quad (80)$$

The pump torque is

$$M_p = \frac{\varepsilon_p V_p \Delta P}{2\pi} + M_{lp} \quad (81)$$

$M_{lp}$  is the hydro-mechanical torque loss of the pump, defined as

$$M_{lp} = f(\varepsilon_p, \omega_p, \Delta P) \quad (82)$$

The oil bulk modulus  $B = 1500\text{Mpa}$ . The pump and motor model can be found in Appendix I and J, the hydrostatic transmission path can be found in Appendix K. Based on the equations of above the dynamic model of the hydrostatic transmission is derived as shown in Figure 6.3.

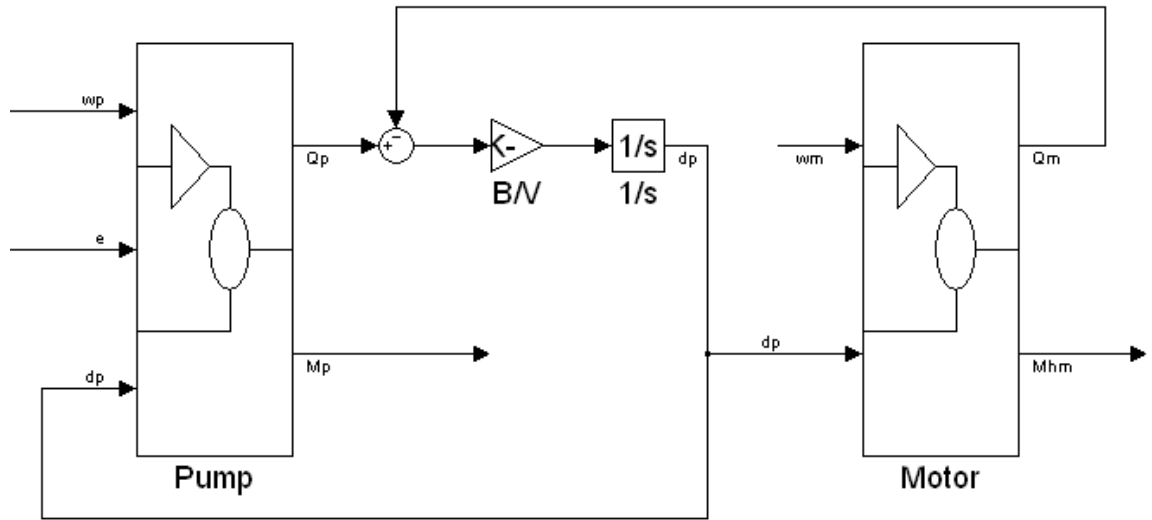


**Figure 6.3** Dynamic model of the hydrostatic transmission

### 6.3 Tire road connection

The slip between tire and road was expressed according to the formula derived by Gustafsson (Gustafsson 1997) as

$$s_l = \frac{v_r - v}{v} \quad (83)$$

Here  $v_r$  is the circumferential velocity of the tire, which is expressed as  $v_r = \omega_w r_w$ , and  $v$  is the absolute velocity.

The friction coefficient is defined based as a function of the traction force  $F_t$  and the normal force  $N$ :

$$\mu = \frac{F_t}{N} \quad (84)$$

$$F_t(s_l) = N \tanh(ks_l) \quad (85)$$

To apply to both positive and negative velocities, the equation was modified as follows:

$$F_t = Gk(v_r, v) = N \tanh\left(k \frac{v_r - v}{|v| + e}\right) \quad (86)$$

$e$  is a constant to prevent division by zero crossing.

### 6.4 Drive wheel model

Figure 6.4 shows the drive wheel model.

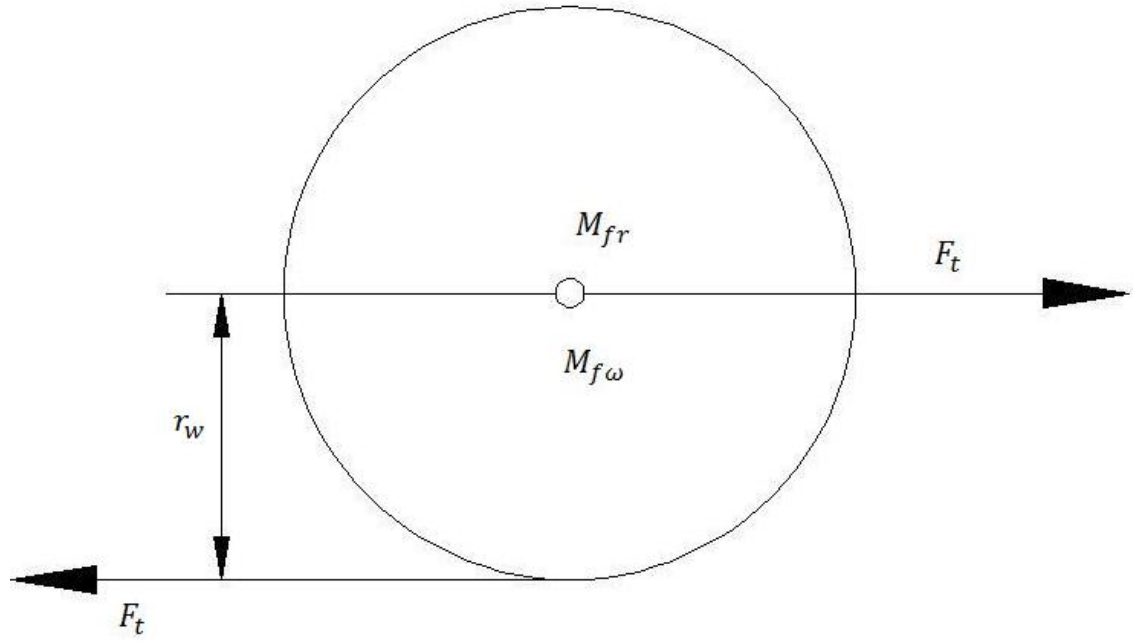


**Figure 6.4** Drive wheel illustration

$F_t$  is the traction force

$M_{fr}$  is the drive torque

$M_{f\omega}$  is the friction torque that is a function of the wheel angular velocity  $\omega_w$  and the constant coulomb friction torque  $M_{f\omega 0}$

$$M_{f\omega} = k_{f\omega}\omega_w + M_{f\omega 0} \quad (87)$$

The driving wheel torque equation can be written as follows

$$\frac{d\omega_t}{dt} = \frac{M_{fr} - F_t r_w - k_{f\omega}\omega_w - M_{f\omega 0}}{j_w} \quad (88)$$

## 6.5 Vehicle dynamics

The vehicle dynamics is illustrated in Figure 6.5



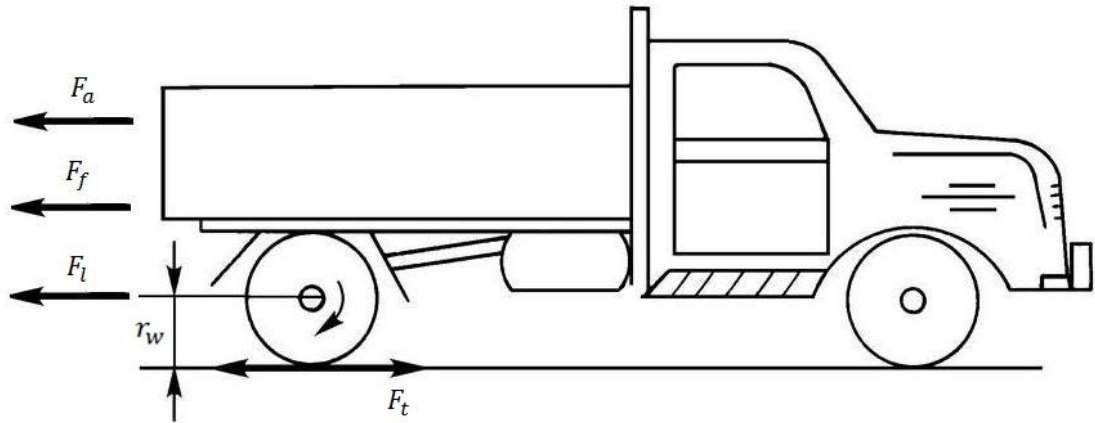


**Figure 6.5** vehicle dynamics

The fraction force of the vehicle is expressed as a function of the velocity

$$F_f = k_{fv}v \quad (89)$$

The vehicle force equation can be written as

$$\frac{dv}{dt} = \frac{(F_t - F_l - k_{fv}v)}{M_v} \quad (90)$$

Here  $F_l$  is the external load force,  $M_v$  is the vehicle mass.

## 6.6 Powertrain model

The powertrain model calculates the velocity of the vehicle  $v$  according to the desired speed of the engine  $\omega_{es}$  and the pump displacement setting  $\varepsilon_p$ , the hydraulic motor angular velocity is defined as a function of  $k_m$  and  $k_{hm}$ . The power train model was based on the simulation model of Huhtala (1996).

$$\omega_{hm} = \frac{\omega_o - k_m\omega_e}{k_{hm}} \quad (91)$$

The drive torque  $M_{fr}$  is the output torque  $M_o$  multiplied by the gear ratio between output shaft and the drive wheel  $i_{fr}$ :

$$M_{fr} = M_o i_{fr} \quad (92)$$

The accessory torque is a function of the engine speed, it can be written as:

$$M_{fa} = 0.0126\omega_e + 20 \quad (93)$$

The engine produces output torque  $M_e$  according to the summation of the mechanically transmitted torque  $M_m$ , the hydrostatic unit driven torque which is the pump torque  $M_p$  multiplied by the gear ratio  $k_p$ , and the torque  $M_a$  that consumed by the accessory devices, which consist of control and flushing pump. The following diagram shows the dynamic model of the hydrostatic-mechanical power split CVT. The details of final can

be found in Appendix E, the engine model can be found in Appendix F, the accessory and planetary gear model can be found in Appendix G and H.

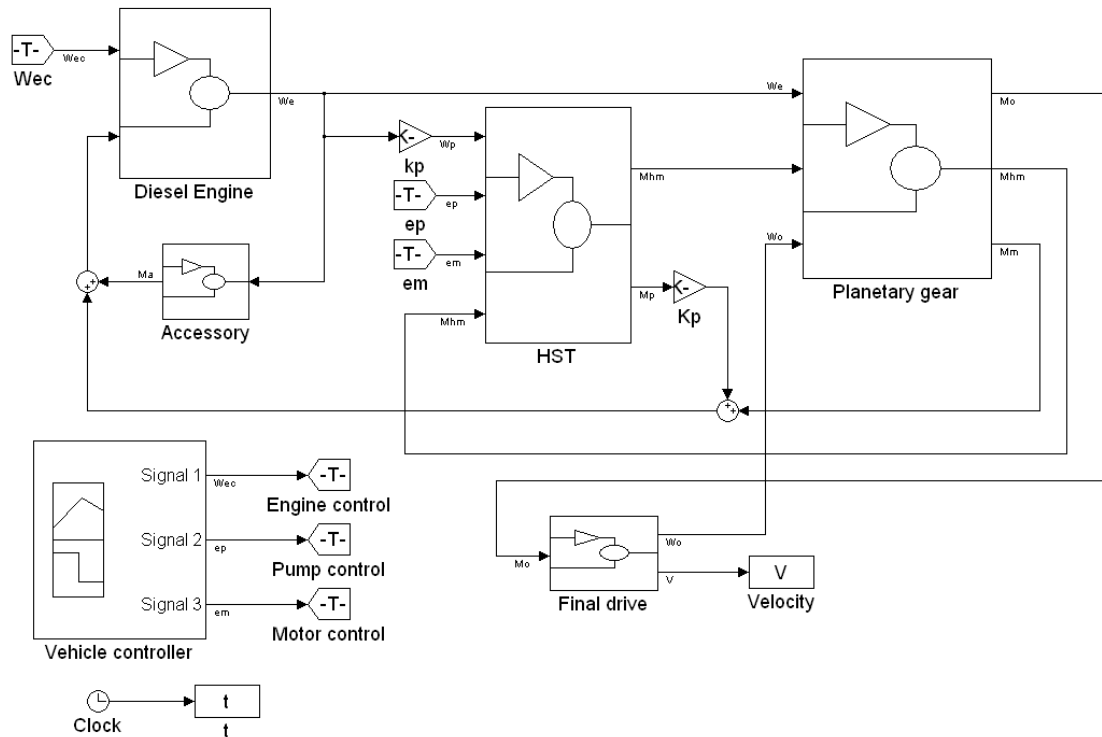


**Figure 6.6** Powertrain model

## 6.7 The powertrain simulation examples

1) The response of the powertrain model to hydrostatic units control signal

**Table 6.1** Powertrain simulation parameters

Simulation parameters	
Engine speed	Constant at 2000rpm
Load	5000N
Pump displacement setting	Changes from 0.25 to 1, then to 0.6

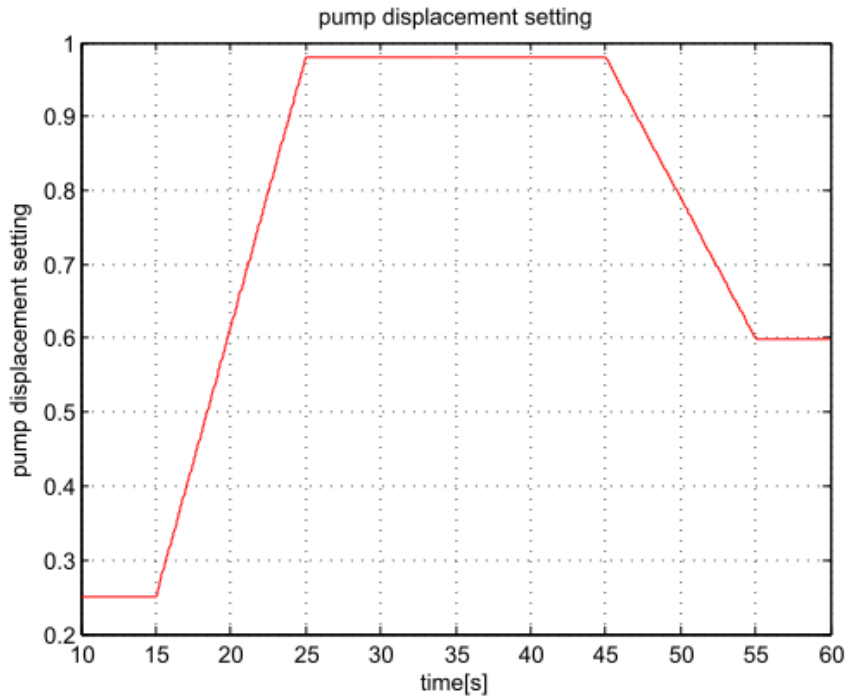


**Figure 6.7** Pump displacement setting

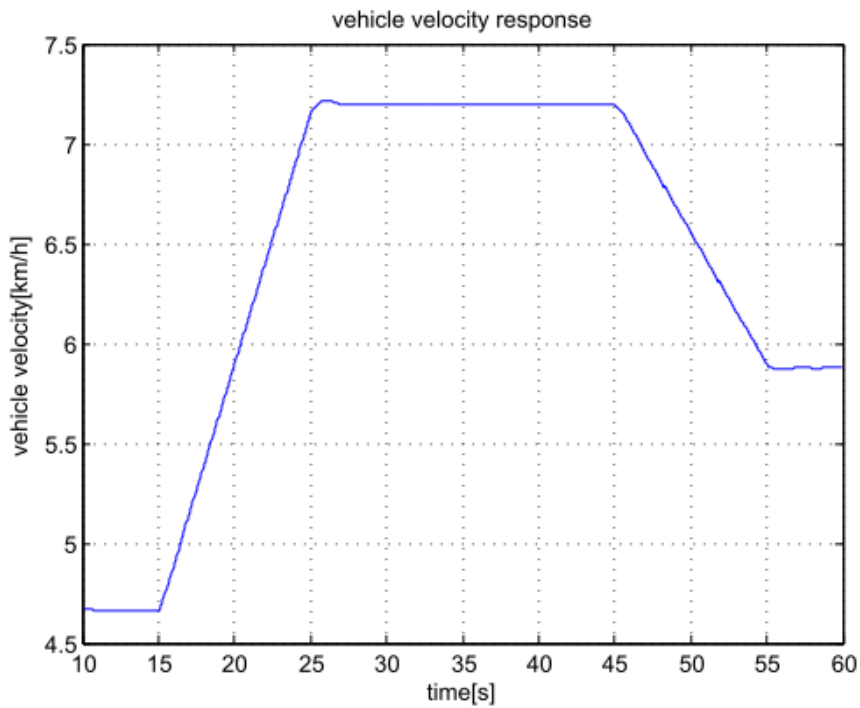


**Figure 6.8** Vehicle velocity response

2) The response of the powertrain model to engine control signal

**Table 6.2** Powertrain control parameters

Simulation parameters	
Engine speed	Changes from 1625rpm to 1997rpm then to 1800rpm

Load	5000N
Pump control	Constant at 1

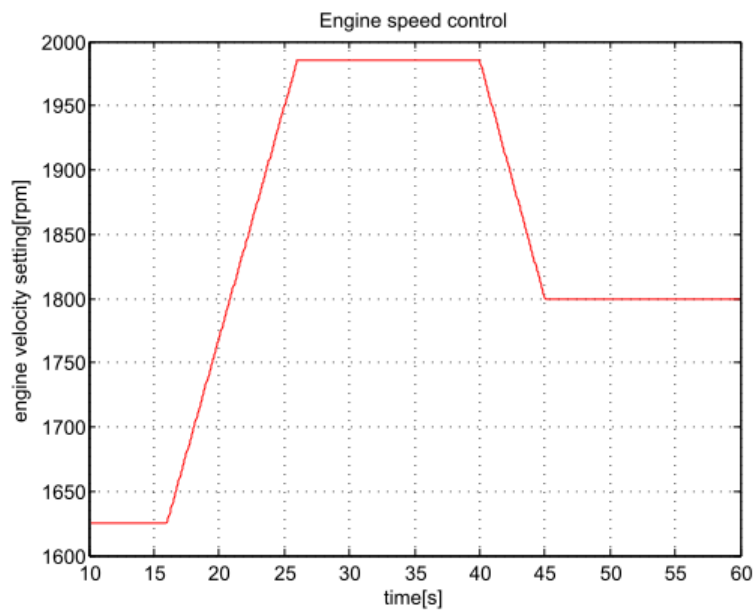


**Figure 6.9** Engine speed control signal

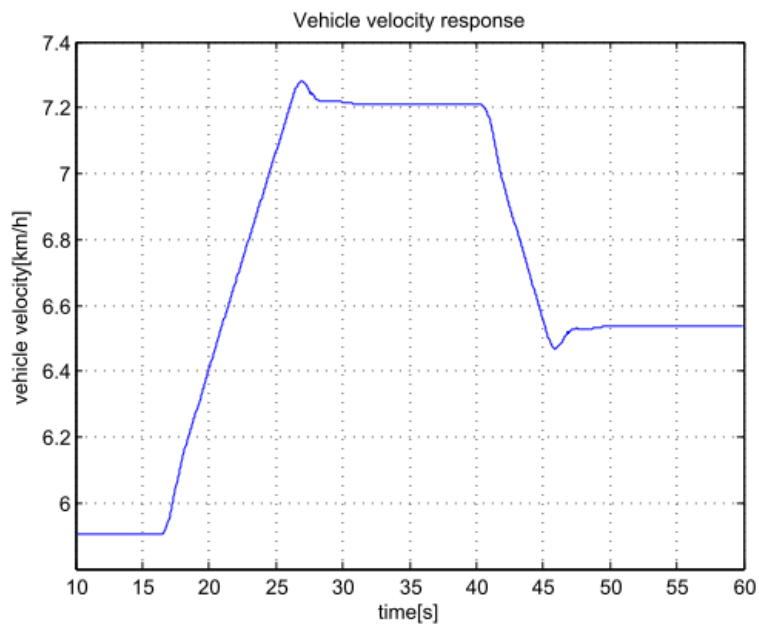


**Figure 6.10** Vehicle velocity response

## 6.8 The working cycle suitability

This study is aimed to find a suitable working cycle under which the hydrostatic-mechanical power split CVT performs best, in other words, the efficiency of the whole working cycle keeps at a high level that can save considerable amount of energy. The typical hybrid vehicle working principle is shown as (Hanyun Yang 2009):

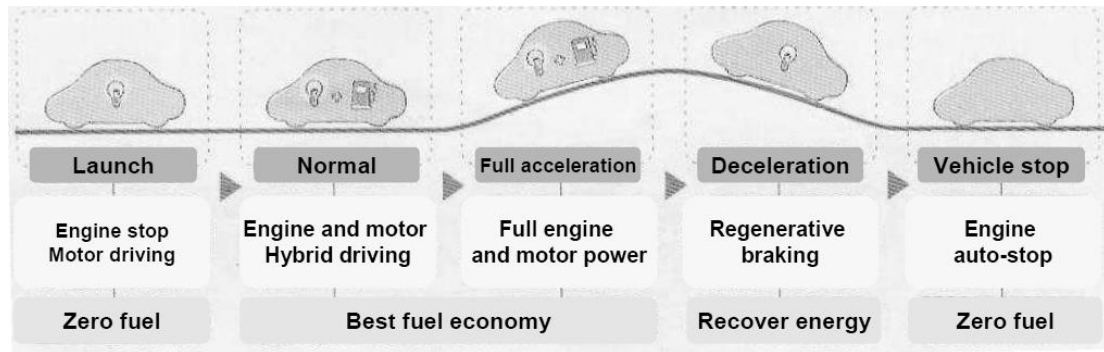


**Figure 6.11** Typical hybrid vehicle working cycle

According to the typical hybrid vehicle working principle of Eaton hybrid solution, the working cycle studied here defined as

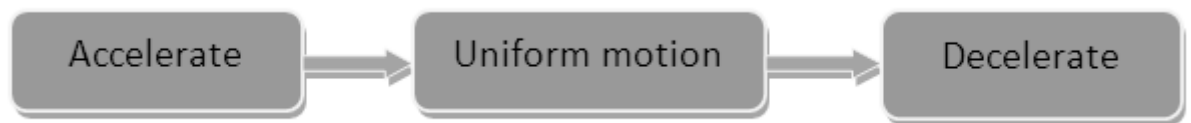


**Figure 6.12** Powertrain simulation working cycle

The simulation parameters of the working cycle study are chosen as

**Table 6.3** Working cycle simulation parameters

Simulation parameters	
Engine speed	2000rpm
Load	5000N
Pump displacement setting	0.75–1–0.7

The simulation result Figure 6.13 and Figure 6.14 show that the efficiency of the transmission keeps higher than 90% during the whole working cycle. The transmission efficiency becomes higher when the portion of the hydrostatic transmission becomes smaller, because at this case more energy is transmitted via mechanical path, which has a higher efficiency than the hydrostatic path.

The *accelerate–uniform motion–decelerate* working mode is widely used by many kinds of transportations such as transit bus, excavator, truck, crane, etc. This means the hydrostatic-mechanical power split CVT technology has great potential to be widely adopted by working machines.

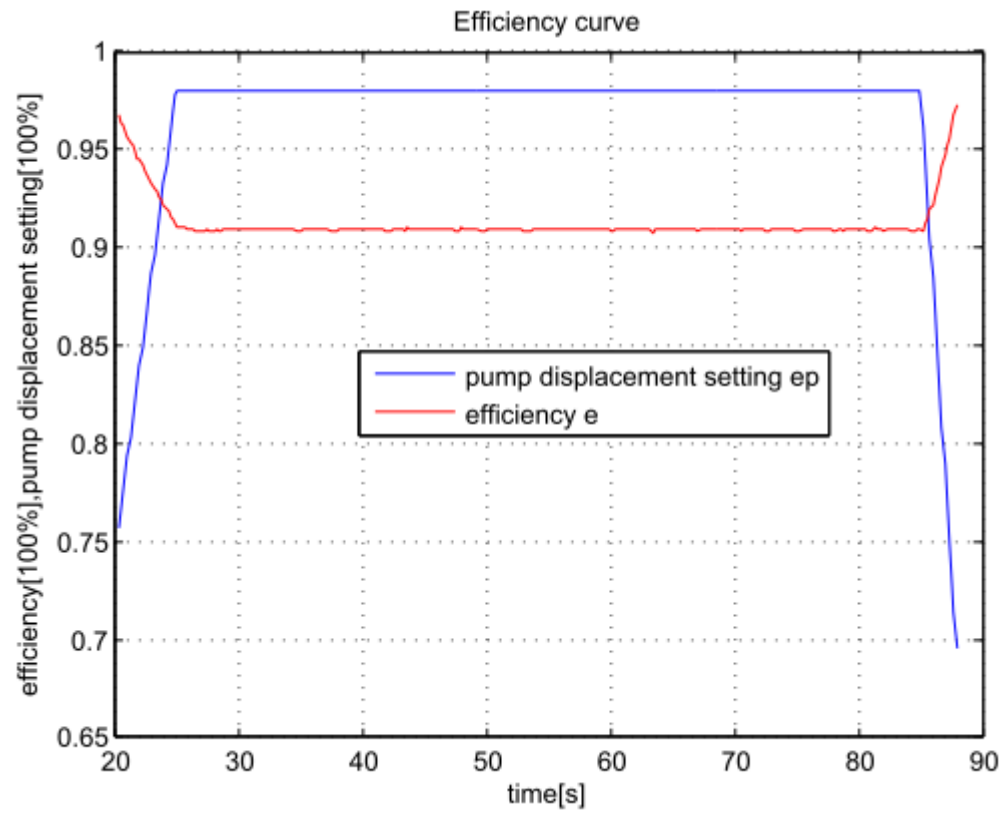


**Figure 6.13** Powertrain efficiency curve

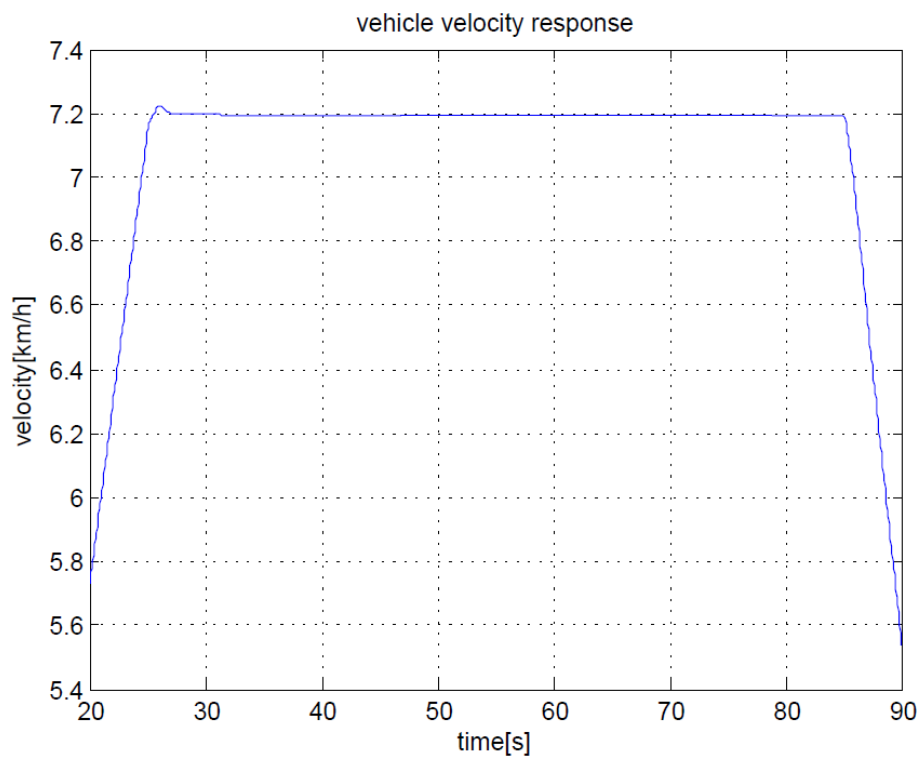


**Figure 6.14** Powertrain velocity response

According to Eaton (Brad Bohlmann 2007), a diesel hybrid hydraulic shuttle bus on a Ford E450 chassis was delivered to the US Army in May 2006. The vehicle met or

exceeded all of the program goals including demonstrating >25% fuel economy improvement on the EPA city driving cycle and reducing in-cab noise during acceleration by more than six dBA. Another Eaton solid waste compaction (refuse) trucks showed the following performance:

**Table 6.4** *Eaton vehicle performance*

	Economy Mode	Productivity Mode
Fuel economy improvement	28%	17%
Vehicle Acceleration	+2%	+26%
Productivity	N/A	+11.5%
Brake Life	>2x	>2x

## 6.9 The power range suitability study

Hydrostatic-mechanical power split CVT systems have much higher power capabilities, in addition to the higher transmission efficiency, they typically regenerate much more braking energy than traditional transmission systems. According to Eaton (Brad Bohlmann 2007), a series hybrid hydraulic UPS truck demonstrated 50-70% better fuel economy than a standard truck.

This study aimed to find the power range suitability of the hydrostatic-mechanical power split CVT technology, power range suitability shows the relationship between engine power range and the total efficiency of the transmission. The power range in this study is 30kW to 120kW. The following table and figure show the simulation result.

**Table 6.5** *Transmission suitability study result*

Engine speed		1600rpm
Hydraulic unit volumetric efficiency		0.88
Hydraulic unit hydraulic-mechanical efficiency		0.88
Engine power (kW)	Torque (Nm)	Efficiency(%)
30	178.6	83.22
35	208.9	84.4
40	238.7	85.83
45	268.5	87.4
50	298.3	87.73
55	328.7	88.83
60	358.3	89.33
65	387.2	89.77
70	417.8	90.17
75	447.5	90.51
80	477.2	90.78

85	507.2	91.11
90	536.8	91.3
95	566.9	91.5
100	596.5	91.65
105	626.5	91.9
110	656.3	92.04
115	686.3	92.16
120	715.6	92.25

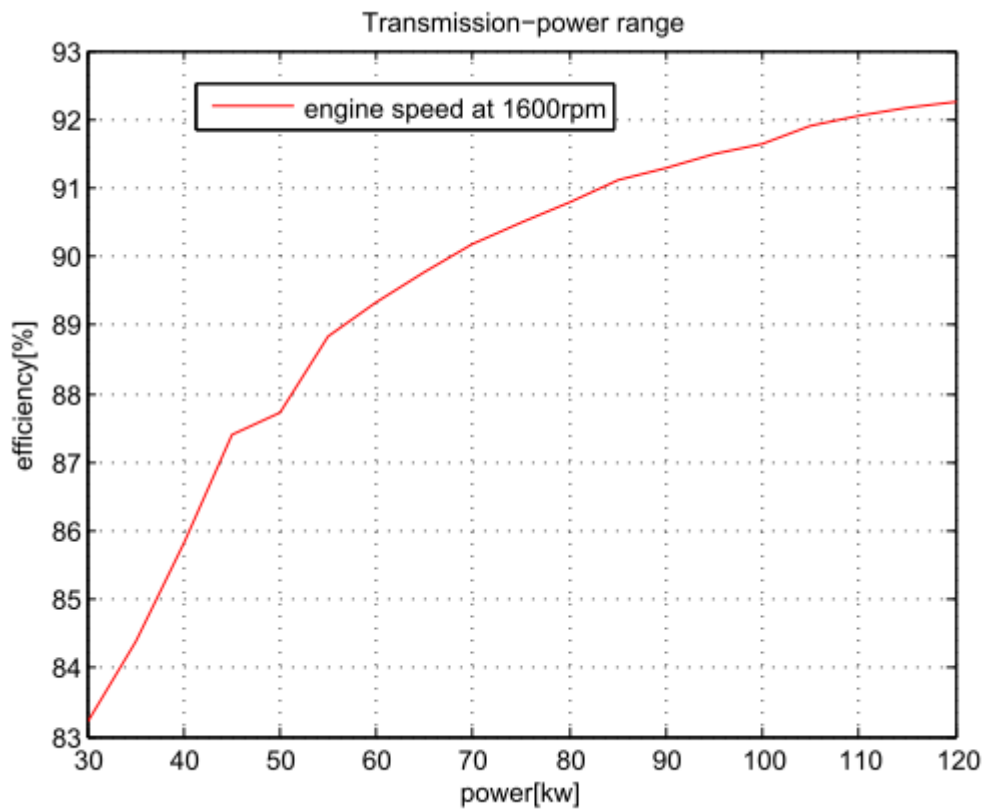


**Figure 6.15** Power range suitability curve

The study shows that the higher the power is applied to the transmission, the better efficiency can be achieved. This means that hydrostatic-mechanical power split CVT technology can be used in most segments of the working machine market, including all light, medium and heavy duty passenger cars, city buses, and delivery trucks. Great potential for application in hybrid technology still remains, the market is still evaluating the technology in many cases.



## 6.10 Conclusion

This study builds a dynamic power-train model of output coupled hydrostatic-mechanical power split CVT. Based on analysis, a normally used working cycle: *accelerate-uniform motion-decelerate* was chose to test the efficiency of the power-train model to test the suitability, the simulation result shows excellent efficiency, this shows hydrostatic-mechanical power split CVT is suitable for machines operate under that working cycle. Then a power-range suitability test carried out based on simulation, the result shows that within the range from  $30kW$  to  $120kW$ , the higher the engine power, the better efficiency is offered by the transmission system, the results shows that hydrostatic-mechanical power split CVT is especially for medium and heavy duty working machines.

In addition, the study result shows that hydrostatic-mechanical power split CVT technology is able to increase the whole system efficiency over that of a signal hydrostatic CVT mode. However, power CVT is difficult to cover the full-required speed range, therefore in practical application additional range gears are needed to increase the speed range.

## 7 Summary

In this study, two general hydrostatic-mechanical power split CVT configurations: input and output coupled hydrostatic-mechanical power split CVT were studied to investigate power split transmission, including the power distribution, the static models, and the steady-state characteristics, to find the advantages and disadvantages of both circuits. Then current applications of the hydrostatic-mechanical power split CVT technology were reviewed to give an idea of how the concept was being used in real product application, and to reveal that there is still great market potential to be explored. Finally, a suitability study was made to show under which working cycle the hydrostatic-mechanical power split CVT offers the best, and under which engine power range the transmission performs best.

The study shows that the lockup point is very important for a power split CVT, the benefits of the lockup point should be considered in practical application to make full use the benefits, for example in heavy duty working speed (6-12km/h). Both principles: input coupled and output coupled systems have advantages and disadvantages, both of them suitable for different applications, so both of the principles are of interesting in practical engineering applications. Overall, hydrostatic-mechanical power split provides better efficiency over traditional hydrostatic CVT, though the design of hydrostatic-mechanical power split CVT is more complex than the traditional hydrostatic CVT. Hydrostatic-mechanical power split CVT is quite suitable for the heavy duty working machines with frequent accelerate and decelerate operations, the higher the power density the better efficiency it will provide.

All the studies were carried out theoretically, practical applications are different from theoretical study results, it is recommend that in real product design a combination of theoretical study and practical test is necessary.

## References

Aitzetmüller Heinz. Steyr S-Matic – The Future CVT System. Seoul 2000 FISITA World Automotive Congress. 2000

Brad Bohlmann. Hybrid Hydraulic System Development for Commercial Vehicles. [WWW]. [Cited 01/09/2010]. Available at: <http://www.aqmd.gov/tao/conferencesworkshops/HydraulicHybridForum/BohlmannSlides.pdf>

Daiheng Ni., Dwayne Henclewood. Simple Engine Models for VII-Enabled In-Vehicle Applications. IEEE TRANSACTIONS ON VEHICULAR TECHNOLOGY, VOL. 57, NO. 5, SEPTEMBER 2008.

Dziuba, F. and R. Honzek. Neues stufenloses leistungsverzweigtes Traktorgetriebe. (A new power-split transmission). Agrartechnische Forschung Vol. 3 No.1: 19-27.1997.

Erkkilä M., Model-based design of power-split drivelines. Doctoral dissertation. Tampere University of Technology publication 825. 2009

Gustafsson, F. Slip-based tire-road friction estimation, Automatica Vol. 33 No.6, 1997, pp.1087-1099.

Hanyun Yang. Eaton Hybrid Solutions: Bus Applications. [WWW]. [Cited 01/09/2010]. Available at: <http://www.modern.ipacv.ro/Eaton%20Hybrid%20Solutions-%20COMPRO%20Final.pdf>

Heera Lee, Hyunsoo Kim. CVT Ratio Control for Improvement of Fuel Economy by Considering Powertrain Response Lag. KSME International Journal Vol 17 No. 11, pp. 1725~1731, 2003.

Huhtala, K. Modeling of the hydrostatic transmission – steady state, linear and non-linear models. Doctoral dissertation. Acta Polytechnica Scandinavia mechanical engineering series No.123, Helsinki, 1996.

Ivantysynova Monika. Design and Modeling of Fluid Power Systems ME 597/ABE 591 -Lecture 15. [WWW]. [Cited 01/07/2010]. Available at: <https://engineering.purdue.edu/Maha/docs/Courses/me597-abe591/Fall2007/ME597-lecture15-07.pdf>

Ivantysynova Monika. Power split drive technology – trends & requirements. Developments in fluid power control of Machinery and Manipulators, 2nd International Scientific Forum, Cracow, Poland 28 June – 2 July 2000.

Jarchow, F. 1981. Hydrostatischmechanisches Stellkoppelgetriebe mit eingangsseitiger Leistungsverzweigung (Infinitely variable hydromechanical couple transmission with

power split at input) German Patent No. 3 147 447 C2. Filed 1.12.1981, granted 14.06.1984.

Kress JH. Hydrostatic power-splitting transmissions for wheeled vehicles - Classification and theory of operation. SAE Paper No. 680549; 1968.

Kevin R. Lang. Continuously Variable Transmissions An Overview of CVT Research Past, Present, and Future. [WWW]. [Cited 01/09/2010]. Available at: <http://www.lasercannon.com/Murano/Files/cvt.pdf>

Marschall, H. 1973. Antriebsvorrichtung, insbesondere für land- und bauwirtschaftlich genutzte Fahrzeuge (Drive concept, mainly for agricultural and construction vehicles). German patent 2 335 629, filed 13.7.1973, granted 30.1.1975.

Molly, H. Hydrostatische Fahrzeugantriebe – ihre Schaltung und konstruktive Gestaltung. Teil I und II. (Hydrostatic vehicle drives - their control and engineering. Part I and II). ATZ Automobiltechnische Zeitschrift Vol. 68, No. 4: 103-110 (I) and No. 10: 339-346 (II). Morris, W.H.M. 1967. The IHC Hydrostatic.).1966.

Norman H. Beachley., Andrew A. Frank. Continuously variable transmissions: theory and practice. College of Engineering, University of Wisconsin, Madison. 1979.

P. Linares., V. Méndez., H. Catalán. Design parameters for continuously variable power-split transmissions using planetary with 3 active shafts. Journal of Terramechanics  
Volume 47, Issue 5, Pages 323-335, October 2010.

Pohlenz, J. and W.-D. Gruhle. Stufenloses hydrostatisch-mechanisch leistungsverzweigtes Getriebe (Continuously variable hydro-mechanical power split transmission). O+P Ölhydraulik und Pneumatik Vol. 46, No. 3: 154-158. 2002

Pablo Noben. A comparison study between power-split CVTs and a push-belt CVT. Technische Universiteit Eindhoven. 2007

Renius, K. Th., Resch, R. Continuously variable tractor transmission. American Society of Agricultural and Biological Engineers, St. Joseph, Michigan, USA 2005, pp.5-37

Renius, K. Th. Tractors. Two Axle Tractors. In: CIGR Handbook of Agricultural Engineering. Vol. III, Plant Production Engineering (edited by B.A. Stout and B. Cheze):115-184.1999.

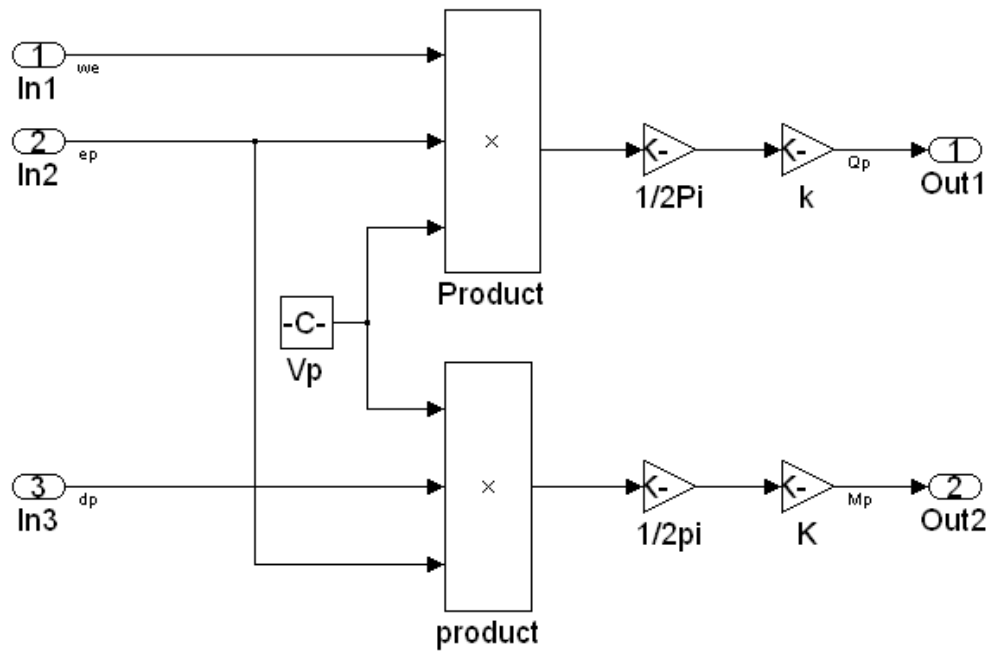
Thoma J., Hydrostatic power transmission, Morden UK, Trade and Technical Press, 1964.

Yuliang Leon Zhou. Modeling and Simulation of Hybrid Electric Vehicles. University of Science and Technology Beijing. 2005

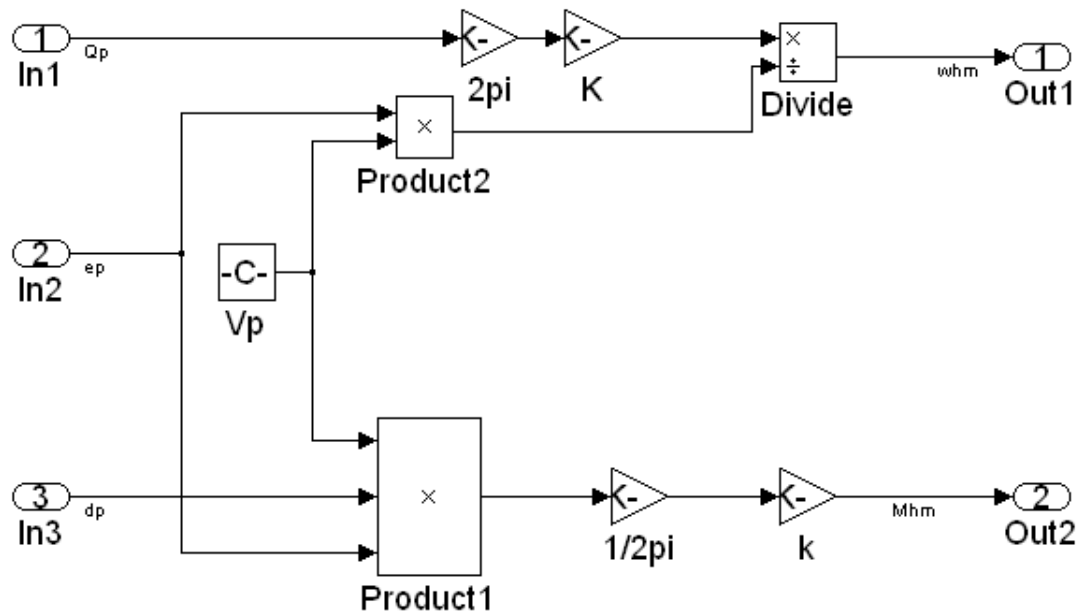
Zbigniew Żebrowski. Hybrid Gears in Farm Tractors. TEKA Kom. Mot. Energ. Roln. - OL PAN, 2007, 7, 321–334

## Appendix: Simulink models

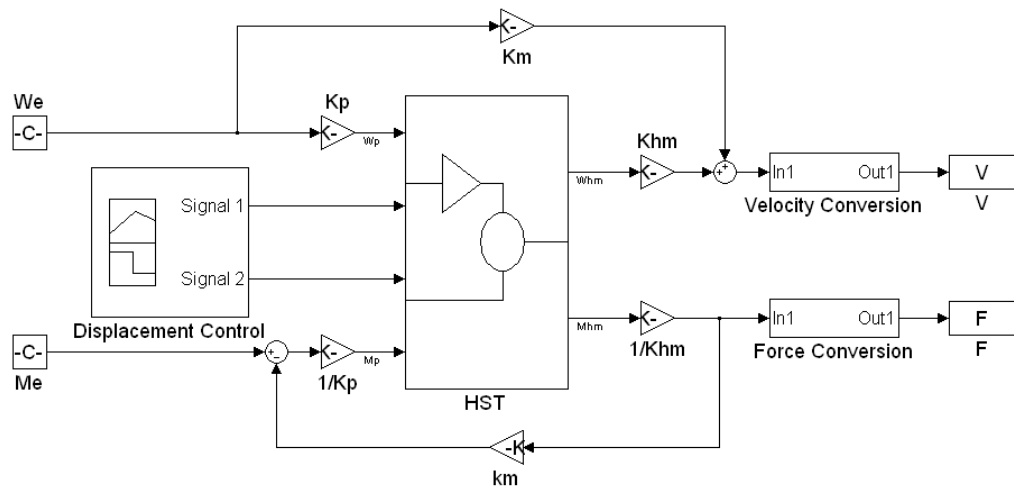
### A. Steady-state ump model



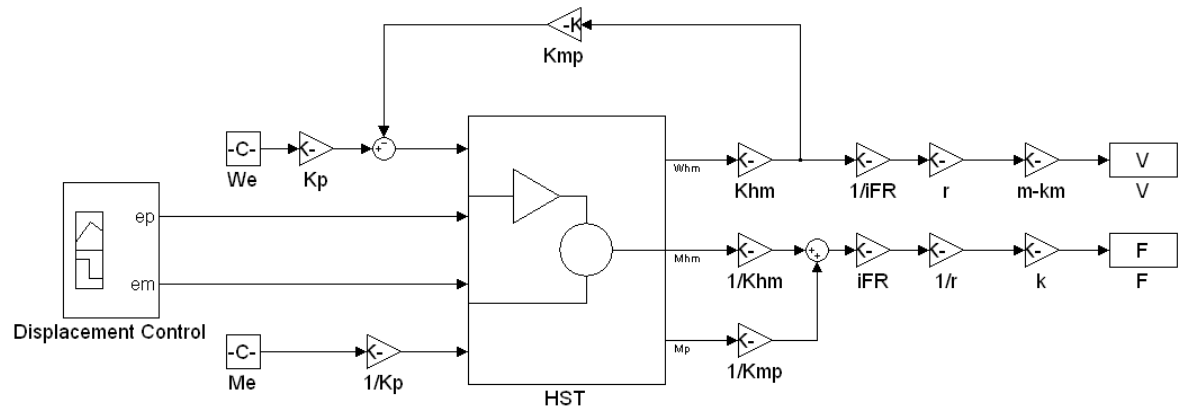
### B. Steady-state motor model



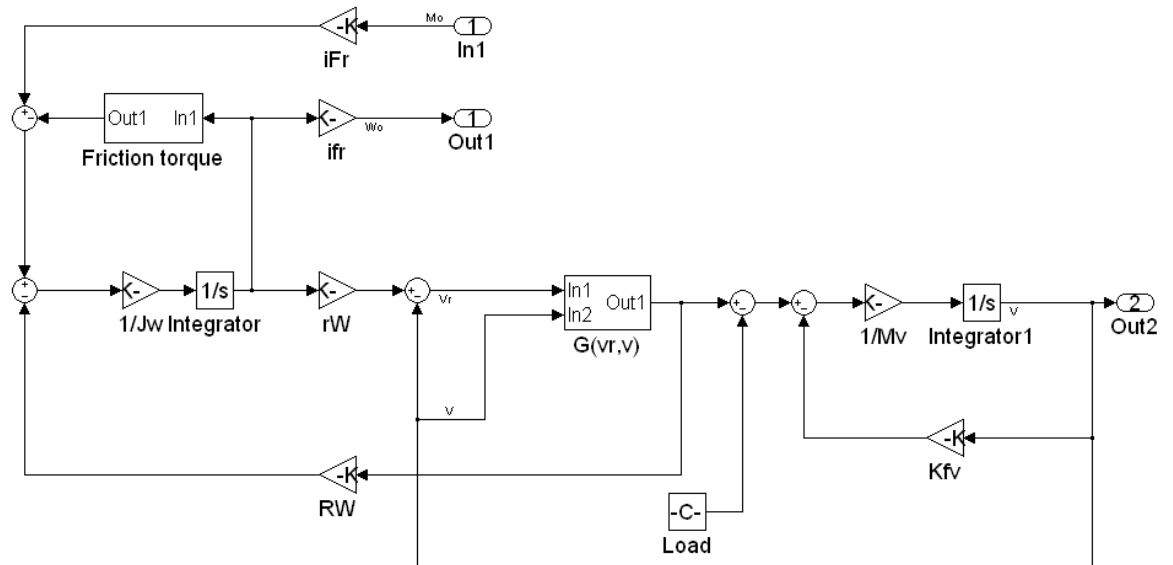
### C. Input coupled steady state model



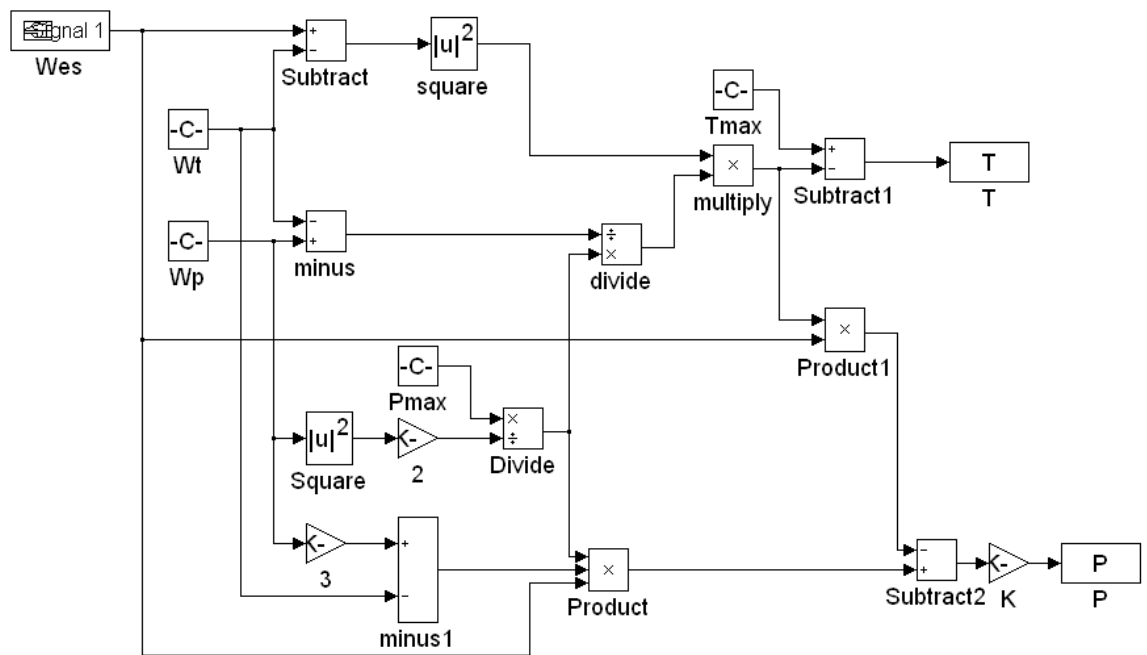
### D. Output coupled steady state model



## E. Final drive

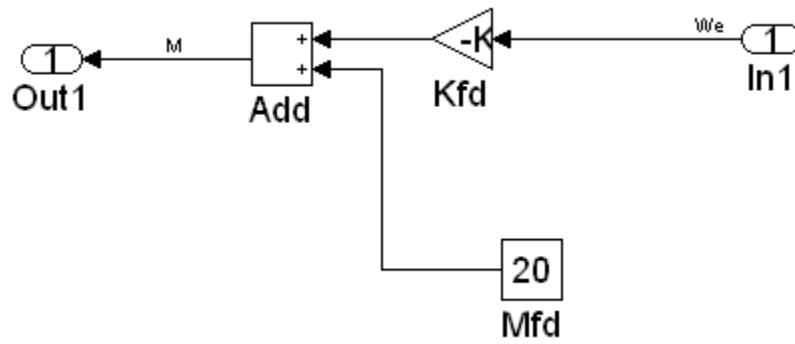


## F. Engine model

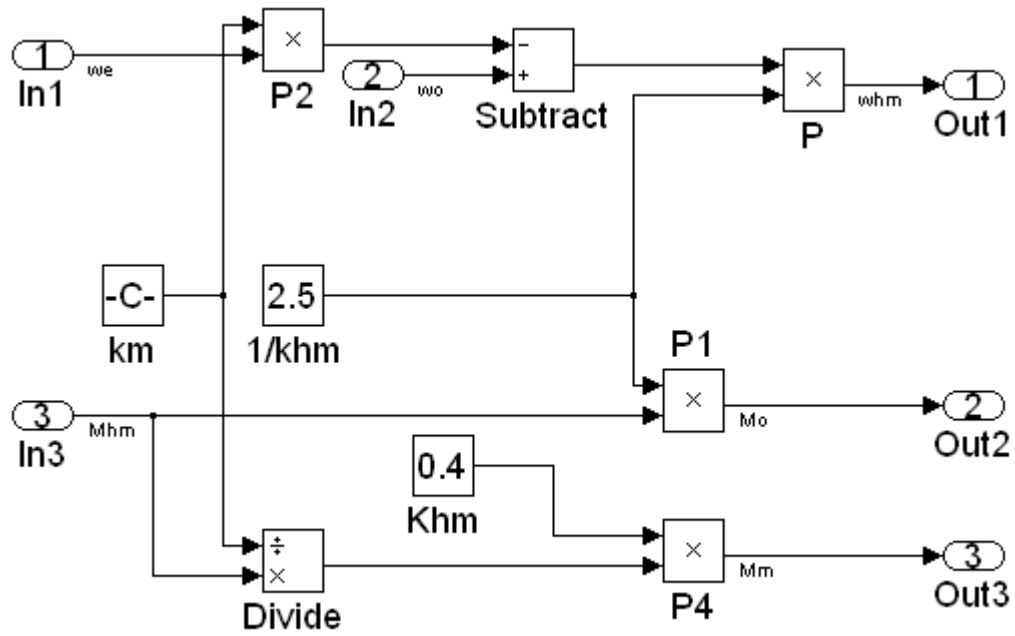




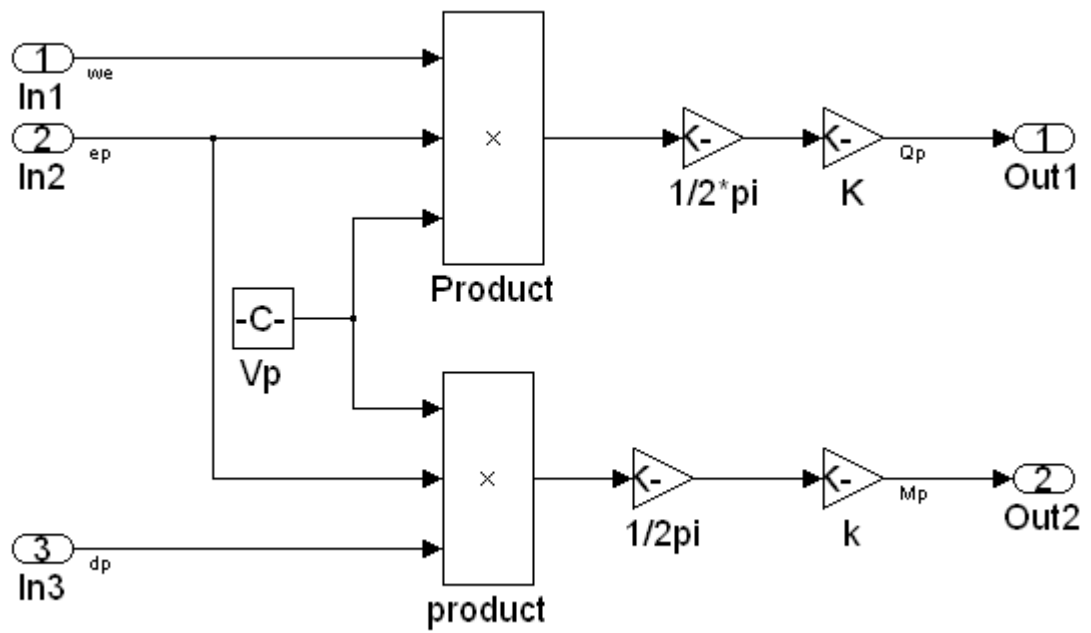
## G. Accessory model



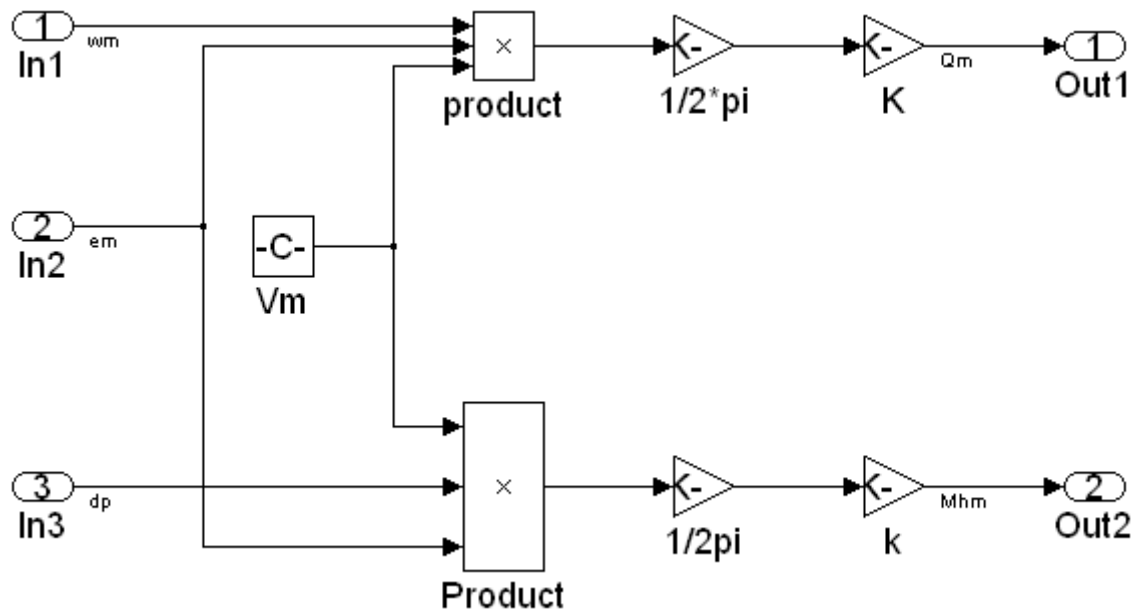
## H. Planetary gear model



## I. Dynamic pump model



## J. Dynamic motor model



## K. Hydrostatic transmission part

